Norges miljø- og biovitenskapelige universitet

Master's Thesis 2018 60 credits

Department of chemistry, biotechnology and food science
Supervisor: Vincent Eijsink

The effects of eggshell membrane on muscle formation in 2D and 3D environments

Eirik Rugstad Haugen
Master-Molecular Biotechnology
IKBM

Acknowledgments

The work presented in this thesis was conducted from august 2017 to June 2018 at Nofima AS at the commodity and research department, located in Ås, Norway. Scientist Sissel Beate Rønning and scientist Mona Elisabeth Pedersen have been my supervisors at Nofima, while Professor Vincent Eijsink was my appointed supervisor at NMBU. This project received financial support from forskningsrådet (NFR 235545).

I wish to express my sincere gratitude to my two supervisors at Nofima, Sissel B. Rønning and Mona E. Pedersen, for giving me the opportunity to work on this project, and for the guidance and encouragement I received during the course of this thesis. I also want to thank Vincent Eijsink for his role as my appointed supervisor at NMBU. I wish to praise the employees of Nofima for being both helpful and friendly during my stay with them, which have made it a truly fun experience working at Nofima. Great thanks to Ragnhild S. Berg for teaching me the ins and outs of the laboratory, to Vibeke Høst for your assistance in my experiments and to Christian R. Wilhelmsen for helping me during my early stay at Nofima.

Finally I wish to thank my parents for their words of encouragements. Andreas Sannerholt and Tor Eirik Hanger for their invaluable assistance in proofreading this text and Magnus Rein for his helpful assistance during these long months, and as a good friend whose coffee drinking has helped me a lot during the writing of this text.

Norges miljø- og biovitenskapelige universitet

Ås 14. 06. 2018

Eirik Rugstad Haugen

Sammendrag

Som en følge av mangel på organer og vev tilgjengelig for transplantasjon har flere personer endt opp med å få sin livskvalitet betraktelig redusert, eller dødd. En mulig løsning på dette problemet er å produsere kunstig vev og organer som kan fylle mangelen. Den mest vanlige måten å danne kunstig vev på er å bruke et biomateriale til å lage en 3D støttestruktur som kan etterligne rollen til den ekstracellulære matriks, som er viktig under vanlig dannelse av vev. Et material som har vist stort potensial er eggeskall membranen (ESM), som deler flere likheter med den ekstracellulære matriksen, og har blitt koblet til forbedringer under sårheling. Dette er egenskapene gjør eggeskall membranen til et lovende biomateriale for å danne en 3D støttestrukturen til produksjonen av vev.

Målet til denne oppgaven har vært å undersøke hvordan ESM påvirket muskelceller isolert fra ytrefilene til nyslaktet storfe i 2D og 3D miljøer.

ESM ble tilført primære muskel celler som pulver eller hydrolysat i 2D miljøer. Pulveret ble tilsatt direkte eller som en komponent i celle-coatingen. Effekten av ESM på proliferasjon, viabilitet og cytotoxitet ble målt med ulike assays, og celledifferensiering ble målt via Real Time-PCR med ulike differensieringsmarkører for mRNA. I 3D forsøk ble muskel celler tillatt å vokse på scaffolds som besto med og uten ESM. Immuno-blotting med fluoriserende antistoffer ble brukt til å studere hvordan cellene interagerte med scaffoldene. Celledifferensiering i scaffoldene ble målt med RT-PCR med ulike differensiering og bindevevs markører.

Resultatene for 2D forsøkene viste at cellene foretrakk å interagere med lave konsentrasjoner av ESM pulver når det ble presenter som en komponent av celle-coatingen. Resultatene viste en nedgang i cytotoxitet, forbedret migrasjons hastighet og tidligere differensiering samt at viabilitet og proliferasjon virket upåvirket. I 3D forsøkene ble det observert at cellene var i stand til å forflytte seg inn i ESM scaffoldene.

Det konkluderes med at måten ESM ble presentert på avgjorde effekten av materialet på muskelcellen. Cellen ser ut til å bli positivt påvirket av ESM i 2D og 3D miljøer, noe som legger til grunne for fremtidige studier for mulige bruksområder til materialet i vev skapelse.

Abstract

A shortage of available tissues and organs for transplantation has led to suffering and death for many people. Tissue engineering could be a possible solution to this shortage, and the most common approach is to use a biomaterial to create a three dimensional scaffold that can mimic the role of extra cellular matrix during *in vivo* tissue formation. A potential material to apply in tissue engineering could be the eggshell membrane (ESM), which share several similarities with the extra cellular matrix, and has been linked to improved wound healing. These properties make the eggshell membrane a promising material for tissue engineering using a 3D scaffold.

The main purpose of this study was to observe the effects of ESM on muscle cells isolated from the sirloin of a newly slaughtered bovine in 2D and 3D environments.

ESM was administrated to primary muscle cells in either powdered or hydrolyzed form in 2D environments. Powdered ESM was added directly or as a component of the cell-coating. The Effect of ESM on proliferation, viability and cytotoxicity was measured using different types of assays. Real time-PCR was used with several differentiation markers to study the effect of ESM on cell-differentiation. During the 3D experiments, cells were allowed to interact with either a pure collagen or ESM scaffold. Immuno-staining with fluorescent antibodies was then used to study cell-scaffold interaction. Differentiation was measured for cells interacting with the scaffolds using RT-PCR with several markers for differentiation markers and connective tissue.

During the 2D experiments we observed that cells preferred to interact with the ESM material when presented as a component of the cell-coating. Further observations showed that ESM had a positive effect on the migration rates for cells, and that cells interacting with the material would seem to enter differentiation earlier. The use of immuno-staining showed that cells were able to migrate into the scaffold.

It was concluded that cell performance was dictated by how ESM was presented. Cells seems to be positively affected by ESM in 2D and 3D environments, which promotes further study into the possible applications for the material in tissue engineering.

Abbreviations

2D	Two dimensional
3D	Three dimensional
ATP	Adenine triphosphate
BGN	Biglycan
$CaCl_2$	Calcium chloride
Col/ Col1A1	Collagen type I
CREMPs	Cysteine-rich eggshell membrane proteins
Dec/ DCN	Decorin
dH_2O	Distilled water
DMEM	Dulbecco's modified eagle medium
DPBS/PBS	Dulbecco's phosphate buffer saline
DSMO	Dimethyl sulfoxide
ECL	Entactin-Collagen-laminin
ECM	Extra cellular matrix
EF-1A/ EEF1A1	Elongation factor 1 alpha
ESM	Eggshell membrane
ESMF	Eggshell membrane fibers
EtOH	Ethanol
FBS	Fetal bovine serum
FN	Fibronection
GAG	Glycosaminoglycan
HA	Hyaluronic acid
HCl	Hydrogen chloride
Hydrol	Hydrolyzed eggshell membrane
Ki67	Kiel 67 (proliferation marker)
LAF	Laminar flow cabinet
LDH	Lactate dehydrogenase
MRF	Myogenic regulatory factors
$MgCl_2$	Magnesium chloride
Mixed ESM	Mixture between coated and hydrolyzed ESM
MSC	Muscle satellite cell
MyoD/ MYOD1	Myogeninc differentiation protein
MYOG	Myogenin
NaCl	Sodium chloride
NCAM	Neural cell adhesion molecule
PAX7	Paired box7
Pen/strep	Penicillin Streptomycin
PG	Proteoglycan
RCF	Relative centrifugal force
RT	Room temperature
RT-PCR	Real time polymerase chain reaction
SEM	Scanning Electron Microscope
TBP/TATA	Tata binding protein
TBS-T	Tris-bufferd saline with Tween 20
WGA	Wheat germ agglutinin

Table of contents

1: Introduction

1.1: A fatal shortage

It is estimated that 20 people will die every day while waiting for a transplant and, as of the writing of this text, a total of 120.000 people were waiting to be accepted for an organ transplant, up from 23.200 during the 90s, based on public data from US department of health and human services. The number of people in waiting will only increase as poor lifestyle choices, such as excessive food consumption, smoking and lack of physical activities take their toll on the population. This is without adding the problems of an increasingly aging world population, that through the effects of *senescence*, which is a weakening of the self-repairing mechanisms of the body and increases the rate of organ failures and tissue degradation, putting an even greater pressure on the transplantation system (Sousa-Victor et al., 2014). Several ideas have been proposed to combat the growing organ shortage; and although many of these ideas have merit, they mostly focus on increasing the pool of available organs, such as an opt-out system. They do not address the underlying problems like organ rejection or the discard of organs due to damage, which cannot be fixed by increasing the availability of donors (Abouna, 2008).

A possible solution to the problem of organ shortage and organ rejection is the engineering of artificial organs which can be transplanted into a recipient. The creation of parts or a whole organ in an *in vitro* environment which can be transplanted into a waiting recipient could provide life improving if not lifesaving treatment. Using the recipients own cells to engineer tissue could remove the issue of transplants being rejected due to incompatibility, and could remove the burden of having to use immune-repressive drugs for the rest of their lives. Tissue engineering could provide a steady supply of available, healthy and compatible organs when needed, and ensure better and safer treatment options than what is currently in use. Often when one thinks of organ donation, it is the donation of vital and complex organs such as heart, lungs and kidneys that comes to mind, however the vast majority of waiting recipients are in need of tissue transplants to replace skin, muscle or heart valves, which may have been lost due to trauma or infection. Engineering vital organs like hearts, lungs and kidneys for transplantation has still not been materialized, but the engineering of tissue such as muscles, skin or even bladder has, and is even being sold on the open marked (Langer & Vacanti, 2016). Engineered skin tissue is already being produced and implemented in over a million people, and several different muscle parts, like cartilage, heart valves, bone and intestine have

been produced *in vitro* (Böttcher-Haberzeth, Biedermann, & Reichmann, 2010). Engineering of tissue has the potential of improving the quality of life for people in need, while also reducing the economic burden on the patient, relatives and society by removing the need for continuous support; and lost revenue due to not being able to function properly in society.

Tissue engineering is a complex and growing field, with several different methods and hypothesis on how to create functional tissue for transplantation and organ engineering. The most common method of tissue engineering is through the use of an artificial 3D scaffold to support and direct cell growth *in vivo* or *in vitro* (Howard, 2008).There are several different factors to take into consideration when engineering tissue, such as how to implement the tissue into the recipient, whether the tissue should be engineered in the damaged area (*in vivo*) or should it be engineered outside of the damaged area and then transplanted in (*in vitro*). There is also the question of what kind of material the scaffold should be made out of, since it is the scaffold that will support and direct the formation of the tissue, selecting the correct material is central, because it determines how the tissue will interact with the scaffold.

This chapter will introduce the reader to some of the basic concepts of tissue design, muscle formation, scaffold design as well as structure and composition of the extra cellular matrix (ECM) and the tested eggshell membrane (ESM) material.

1:2: The skeletal muscle

The skeletal muscle is one of three main categories of muscles found in the human body, with the other two being smooth and cardiac; together they make up 45% of the total body mass of a healthy human (Ostrovidov et al., 2014). There are also several intermediate variations between all these three categories, adding to the complexity of the muscle system (Alberts, 2017) . This complexity is reflected in the vast amount of different functions that muscles are involved in; skeletal muscles alone are involved in ocular motion, metabolism, locomotive motion and injury response, etcetera and is essential for proper daily functions (Ostrovidov et al., 2014). Even with a large number of different functions and structures, there are similarities with how skeletal muscles are constructed, with several different components working together to create movement. The primary component is the fiber, which consist of several myoblast cells that fused together during myogenesis, forming a long multinucleated unit that can contract when stimulated (Ostrovidov et al., 2014). Several of these fibers are bundled together in small groups forming the *fascicle*, and several of these *fascicles* are then

capsulated by the *epimysium*, forming the primary body of the muscle (figure 1.2) ("Structure of the skeletal muscle ", accessed 2018). Inside the muscle there are three layers of ECM that protect and provide structural support; these are the *endomysium*, *perimysium* and *epimysium* (Lieber, 2011). The *endomysium* separates the different fibers from each other inside the *fascicles*, while the *perimysium* encapsulates the different *fascicles* and separates the *epimysium* from the *fascicle* (Lieber, 2011). There are other components of the muscle such as blood vessels that transport nutrients and remove waste, and the *tendon* which binds the muscle to the skeletal structure (Ostrovidov et al., 2014).

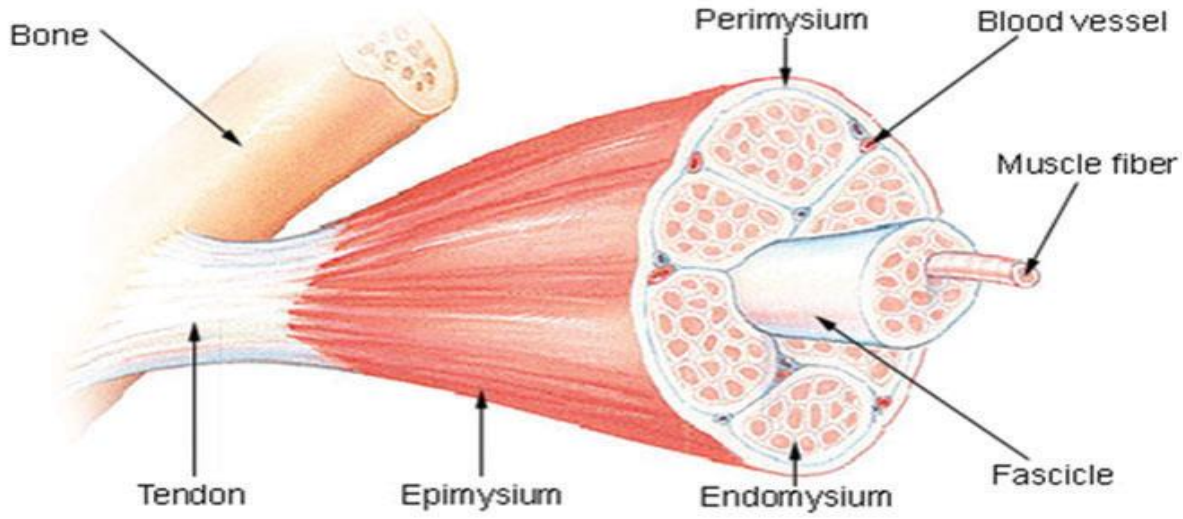

Figure 1.2: Structure of the skeletal muscle. *Illustrated overview of the skeletal muscle, important components of the muscle is highlighted in black.* ***Figure was reproduce from (Ostrovidov et al., 2014).***

1.2.1: Skeletal muscle regeneration

Muscles are constantly susceptible to major and minor damage, from the daily wear and tear to major trauma, the body must be able to regenerate damaged or lost tissue; if unable, severe handicap or even death could be the result. The regenerative system can be divided into two parts; the degenerative and regenerative phase. The degenerative phase is initiated by necrosis, which is a result of damaged tissue being broken down naturally with cells dying due to damage or through enzymatic digestion, which helps to prepare the area for the next phase (Charge & Rudnicki, 2004). The removal of damaged tissue is followed by the activation and recruitment of inflammatory and myoblast cells which assist in the repair and protection against unwanted contaminations (Charge & Rudnicki, 2004). The first inflammatory cells that accesses the damaged area are neutrophils, followed by macrophages;

the recruitment of inflammatory cells are considered important threshold of muscle regeneration, and marks the early part of next phase, the regeneration phase (Tidball, 2005). The arrival of macrophages will mobilize ECM secreting cells such as myoblast and fibroblast cells by releasing several different proteins that promotes migration and proliferation in the damaged area (Frantz, Stewart, & Weaver, 2010). With the recruitment of inflammatory and myoblast cells, the second part of muscle regeneration can begin. The regeneration phase begins with the proliferation and differentiation of myoblast to be used in muscle repair (Charge & Rudnicki, 2004). There are several similarities with regeneration and early embryonic development of muscle, with myoblast starting to differentiate and fuse together with existing fibers for regeneration, or with each other to form totally new fibers (Charge & Rudnicki, 2004). Unlike early embryonic muscle development, the regeneration process is dependent on damaged tissue still having a partially intact ECM to function as a template for muscle regeneration (Bentzinger, Wang, & Rudnicki, 2012). During the regeneration process, new ECM will be produced by myoblast and fibroblast cells through secretion of different ECM components such as collagen, fibronectin and hyaluronic acid which will be used to synthesis or to repair damaged ECM (Frantz et al., 2010). The new ECM will go through several phases of remodeling until reaching maturation at the end of the regeneration process. This remodeling can be observed with an increase in cell-matrix interaction after a period of time, often over several days (Goetsch, Hawke, Gallardo, Richardson, & Garry, 2003). The correct remodeling of the ECM is essential for muscle architecture, and faulty remolding can lead to scarring and loss of function in the associated muscle (Goetsch et al., 2003).

1.3: Muscle satellite cells

Muscle satellite cells (MSC) are quiescent, myogenic committed cell that activates when muscle tissue is damaged or stressed, and is the main source of cells for postnatal formation of new muscle tissue (Cossu & Biressi, 2005; Yablonka-Reuveni, 1995). The English Medical Dictionary defines MSC as “a mononuclear undifferentiated cell that is found in skeletal muscle fibers and promotes their growth, repair, and regeneration”. The MSC are located in small clusters between the basal lamina and the fiber plasma membrane, these clusters are formed during late stage fetal development from progenitor populations of undifferentiated myoblast cells (Le Grand & Rudnicki, 2007). Satellite cells during the later stages of fetal development myoblast progenitor cells will migrate and position themselves in areas around the newly formed myofiber and produce small clusters of myogenic committed stem cells that will form the MSC cluster (Le Grand & Rudnicki, 2007; Yablonka-Reuveni, 1995). The MSC

cells will lie in a quiescent state until activated. When activated the cells will start to generate myogenic committed daughter cells that will emigrate out of the cell pool towards the target area where they will proliferate and differentiate into new tissue. It has also been proven that these daughter cells can enter into several different mesodermal lineages like bone and fat (Bentzinger et al., 2012; Le Grand & Rudnicki, 2007). Not all cells will migrate out of the cell cluster: around 20% of all MSC will remain and regenerate the MSC cluster with new cells so that the number of cells remains constant (Bentzinger et al., 2012). When cells start to differentiate they will migrate towards each other and fuse in an end-to-end structure, and then more cells will be added to each end until a long multicellular structure is formed, this is the myotube, several myotubes while then fuse together and form a muscle fiber (Bentzinger et al., 2012). There are several similarities between muscle satellite cells and myogenic committed stem cells such as common transcription factors, signaling molecules, the ability to generate tissue and regeneration. However, MCS has the ability to move in and out of quiescent state and regenerate its own cell population (Bentzinger et al., 2012). It has also been shown, due to difference in expression for the myogenic regulatory factors that MSC and stem cells are two different lineages of cells (Bentzinger et al., 2012; Sabourin & Rudnicki, 2000).

1.3.1: Activation and function of the Satellite muscle cell

The MSC are activated by the occurrence of damage or stress to the muscle tissue, and migrates toward the damaged area to assist in repair and regeneration of new tissue. With the activation of MSC two pathways open up to the cells, they can either migrate to assist in the repair and regeneration process, or return to a quiescent stage where they will assist in replenishing the cell cluster with new MSC that can be used if any further damage occurs (Verdijk et al., 2014) The activation pathway of the quiescent MSC are believed to differ after the type of tissue the MSC cluster belongs to, and the kind of damage that have occurred (Le Grand & Rudnicki, 2007). However, the notch signaling pathway is believed to be the most common used pathway for the activation of the MSC, and that it is the surrounding muscle tissue that activates the MSC cluster through the expression of several different activation factors (Le Grand & Rudnicki, 2007; Yablonka-Reuveni, 1995). When MSC are in the quiescent phase, several different cellular processes are downregulated, however certain surface proteins and Pax7, which is essential for the maintenance and renewal of the MSC, are continuously expressed to ensure that cells are maintained and functional (Yablonka-Reuveni, 1995). Activated MSC that are myogenic committed to muscle regeneration goes through four

distinct phases with the different myogenic regulatory factors and Pax3/7 being up or down regulated between each phase (figure 1.3.1); these phases are referred to as myogenesis and will eventually turn the MSC into muscle cells though differentiation. Myogenesis is regulated by the myogenic regulatory factors (MRF) myoD, myogenin, myf-5 and MRF4 which convert non muscle cells into muscle cells, making the MRF important for the correct formation of muscles (Ostrovidov et al., 2014). During activation and proliferation the myogenic regulatory factors MyoD, which regulates differentiation, and Myf5, which regulates proliferation and homeostasis, are expressed together with Pax7 and Pax3 (Le Grand & Rudnicki, 2007). During differentiation myogenin and MRF4 becomes up-regulate, myogenin and MRF4 assists in the formation of myotubes and cell differentiation (Le Grand & Rudnicki, 2007). For cells to enter differentiation they will first have to exit the proliferation phase due to proliferation and differentiation being exclusive events (Ostrovidov et al., 2014).

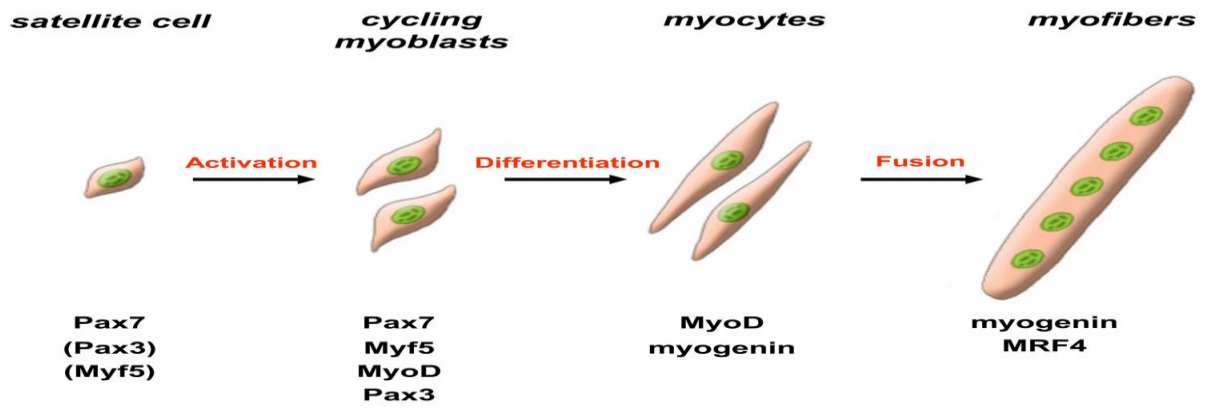

Figure 1.3.1: The expression of different genetic factors during MSC myogenesis. *Change in expression of different genes from quiescent MSC to fully functional myofibers. Figure was published in, and reproduced from (Le Grand & Rudnicki, 2007)*

1.3.2: Myogenesis and the myogenic regulatory factors during tissue regeneration

Myogenesis is regulated by the myogenic regulatory factors (MRFs) which belongs to a superfamily of transcription factors which shares a basic helix-loop-helix domain (Berkes & Tapscott, 2005). There are has four identified members: MyoD, myogenin, myf-5 and MRF4, which can be divided into two groups, the primary MRFs (MyoD and myf-5) and the secondary MRFs (myogenin and MRF4) (Sabourin & Rudnicki, 2000). The primary MRFs are needed for proliferation, differentiation, and homeostasis, with differentiation being regulated by MyoD while proliferation and homeostasis is regulated by myf-5 (Le Grand &

Rudnicki, 2007). The secondary MRFs have been shown to be essential during muscle determination, terminal differentiation and myoblast fusion with myogenin being essential for the formation of myotubes (Sabourin & Rudnicki, 2000). The role of MRF4 in myogenesis seems to not be completely understood, as inactivation of MRF4 leads to the up-regulation of myogenin and the formation of normal muscle tissue, however the expression of MRF4 seems to be closely related to the formation of myotubes (Sabourin & Rudnicki, 2000). Activation of the different MRFs happens at different points during muscle regeneration, with no visible expression of any MRFs during the quiescent stage for MSC, however upon activation of the MSC due to trauma or injury, MyoD or myf-5 is quickly upregulated coupled with the down-regulation of Pax 3/7, leading to the production of myogenic committed daughter cells that can enter into myogenesis (Sabourin & Rudnicki, 2000). MSC seems to be able to enter into myogenesis by expressing either MyoD or myf-5, however during proliferation both genes are co-expressed, and the lack of either gene have been related to the formation of malformed and even missing muscle structures (Sabourin & Rudnicki, 2000). The next MRFs to be activated are myogenin and MRF4, these two MRFs are essential for the formation of myotubes and of the fusion into muscle fiber (Sabourin & Rudnicki, 2000). Though several different factors unrelated to the MRF have been shown play a central role during proliferation and differentiation, such as desmin, the activation and regulation of a satellite cell is primarily controlled and regulated by the MRFs, with an increase in expression of MyoD marking the beginning of differentiation, while an increase in the expression of myogenin is related to myotube formation (Rønning, Pedersen, Andersen, & Hollung, 2013; Sabourin & Rudnicki, 2000). As previously mentioned the downregulation of certain MRF can be handled by the cell by up-regulating the expression of other MRFs, cells lacking myf-5 have been shown to up-regulate MyoD expression and vice-versa, which would lead to normal but delayed muscle formation (Hernández-Hernández, García-González, Brun, & Rudnicki, 2017). Cell lacing MRF4 can up-regulated myogenin expression and normal tissue would form, however cells lacking myogenin could not form normal muscle tissue by up-regulating MRF4, which could show that there is a certain redundancy between the different MRFs (Hernández-Hernández et al., 2017). It has been speculated that the four MRFs originated from a single MRF-gen, with myf-5 representing the ancestral gene, and that the new genes evolved as a result of the complex musculature of higher organisms (Hernández-Hernández et al., 2017).

1.4: The fundamentals of tissue engineering

Tissue engineering is the production or engineering of new tissue inside or outside of an organism, using living cells. The term tissue engineering was first formulated during a national science workshop in 1988, and was defined as “the application of principles and methods of engineering and life science toward the fundamental understanding of structure-function relationship in normal an pathological mammalian tissues and the development of biological substitutes to restore, maintain or improve tissue function” (O'brien, 2011). There have been several breakthroughs in tissue engineering since the term was first coined with the engineering of skin, muscles and bladder (Howard, 2008). The modern field of tissue engineering has developed into a multi-disciplined research field that incorporates life and medical sciences with engineering and material sciences to produce functional tissue for human needs. The engineering process requires the interaction and integration between cells so the tissue can be correctly formed, therefore any process that tries to engineer tissue is depended on being able to integrate different modifying factors during the process (Howard, 2008) There are two main approaches to the use of scaffolding in tissue engineering. The first approach is to use the scaffold to promote regeneration of tissue by implanting it directly into a target area *in vivo*, assisting the natural formation of new tissue (Howard, 2008). The second approach is to use the scaffold to grow tissue *in vitro* that can then be transplanted into the target area (Howard, 2008).Though the two methods differ in their execution, their primary endpoint is similar, with the formation of new tissue and the degradation of the artificial scaffold with the formation of new native ECM that can support the newly formed tissue (Howard, 2008). When engineering tissue *in vitro* there are several different factors that needs to be taken into consideration, such as how to transplant the engineered tissue into target area, what kind of material to make the scaffold out of, and how cells should be implemented onto the scaffold.

1.5: Scaffold for tissue engineering

A scaffold is a 3D structure made out of a degradable biomaterial which has an interconnectivity porous network structure that cells are able to migrate through (O'brien, 2011). Designing a scaffold for tissue engineering can be difficult due to the many different functions that the scaffold must be able to support during tissue formation, most designs as of today tries to use material that mimic the composition of the ECM, as it is often considered the optimal scaffold due to its role in tissue formation and regeneration *in vivo* (Ohto-Fujita et al., 2011). It is also preferable to engineer tissue in 3D scaffolds rather in a 2D environment due to the fact that a 3D system more closely mimic the natural environment of most tissue, making it easier to structure the tissue correctly, which in return makes the tissue more identical to its natural formed counterpart (Ohto-Fujita et al., 2011) . Several different materials have been proposed, as a possible replacement for the ECM, with the majority being either biological or synthetic polymers such as collagen or polyester (Chen, Ushida, & Tateishi, 2002). The usage of biological polymers have often been difficult due to the lack of control in enzymatic degradation and poor structural performance, while the usage of synthetic polymers have proven to lack biocompatibility and some materials are not even biodegradable, remaining in the tissue which have been shown to be causing inflammatory responses (Chen et al., 2002). Still with all of these different materials to choose from, there are still some shared requirements that most scaffolds should fulfil before it can be considered desirable for tissue engineering.

1: Scaffold material should be **Biocompatible**, meaning cells must be able to survive within the scaffold without dying or suffer reduced functionality. This implies that cells should be able to migrate, adhere and proliferate inside the scaffold in a similar fashion of ECM. The scaffold should also not illicit an immune response when implanted into a host as it could induce an inflammatory response ,which in return could compromise the tissue and the regeneration process (Chen et al., 2002).

2: The material must be **Biodegradable** in such a way that the cells or the organism is able to break down the scaffolding while new ECM is produced to replace the disappearing scaffold. It is also important that the waste product of the scaffold is not toxic, as it could induce an immune response or damage the organism (O'brien, 2011).

3: The **mechanical properties** should mimic the indented area of implantation so that the cells are both structured and act correctly. Cells should be able to easily migrate inside the scaffold without physical obstruction or hindrance. The mechanical properties should be made so that the scaffold is able to withstand physical pressure without breaking, making it possible to move the scaffold from *an vitro* to *an vivo* environment if needed, or to withstand pressure from the surrounding tissue (O'brien, 2011).

4: The **architectural** design of the scaffold should optimize waste removal, so that waste does not accumulate inside the scaffold. Nutrition should also be easily accessible to cells. The design of the scaffold should not interfere with surroundings tissue in such a way that it affects the structure of that tissue (O'brien, 2011).

5: Production capacity, while this factor does not affect the quality of the scaffold and its effect on the body, the material used for scaffold design should be easy and cheap to produce, as limitations in production will reduce the availability of the scaffold itself, and as a result the scaffold would become less useful (Chen et al., 2002).

A material that share several of these requirements could be considered functional for tissue engineering, however some of these requirements are more important than others, such as a scaffold being biocompatible and biodegradable due to how tissue engineering is implemented, with the scaffold often being either implemented *in vivo* into the damaged area to assist in tissue regeneration, or *in vitro* with tissue being engineered outside of the damaged area and then transplanted into the desired body part (Böttcher-Haberzeth et al., 2010). The formation of tissue is a complicated process that involves several different cell types at different stages of development, and it is therefore important that the scaffold is able to interact with these of cells correctly, while ensuring that the formation of tissue is accurate (Ma et al., 2011). There are several different methods used to mimic correct interaction between cells and the scaffold, from rolling bottle culture, that ensure homogeneity in the cell culture, to layered scaffolding that consist of different components which initiated different biochemical cues to the cells as the scaffold is broken down (Ma et al., 2011). For the formation of advanced tissue such as muscles, it is important that the scaffold promotes vascularization, as it is essential for the correct function and formation of the tissue.

Vascularization, or the formation of blood vessels, ensures that nutrition is accessible, while waste products are removed during and after tissue formation (Ma et al., 2011).

Overall it is desirable that the 3D scaffold used for tissue engineering mimic that of the ECM, and particularly the ECM of the native tissue on which to engineer. The primary reason for mimicking the ECM is that it is preferable that cells interact with the scaffold material in a similar fashion to how the cells would have interacted with the ECM in normal *in vivo* conditions, making it more likely that the engineered tissue will from and act correctly (Ostrovidov et al., 2014). It has therefore often been preferable to use materials that share similarities in composition and structure to that of the ECM when creating a 3D scaffold, which may be able to more correctly mimic the natural signaling and interaction pattern between the cell and the ECM found in the native tissue (Ostrovidov et al., 2014). When cells interact with the scaffold, they will extend a filopodia to probe the layout and guide cell migration, many different approaches to scaffold design tries to take advantage of this feature (Ostrovidov et al., 2014). There are already several different types of 3D scaffolds available worldwide, which have been designed for different types of tissue like skin, bladder, nerve and bones with different types of biomaterials making up the 3D structure (Chen et al., 2002).

1.6 The Extra cellular matrix

All types of tissue have an extra cellular matrix (ECM) that consists of non-cellular components and provide support, initiate important biological processes such as cell proliferation, differentiation and morphogenesis as wells as protecting cells and tissue from unwanted contaminations (Frantz et al., 2010). The ECM is important for maintaining normal cell functioning and homeostasis, some diseases, such as cancer and fibrosis, have been shown to originate with changed composition in the ECM (Bonnans, Chou, & Werb, 2014). The ECM is for the most part made up of several different fibrous proteins, proteoglycans, glycoproteins and large amount of water, with some differences in composition and function based on what kind of tissue the ECM belongs to (Frantz et al., 2010). The main structural element of the ECM is the fibrous network buried throughout the ECM, which network consist of collagen type I and III together with elastin and fibronectin (FN) which is encapsulated by an hydrogel consisting of PGs (Frantz et al., 2010). Proteoglycans (PG) is a component of the ECM, which meditates cell behavior and ECM composition, and further provide structural integrity and support during ECM formation and tissue regeneration

(Lieber, 2011). There are several different fibrous proteins in the ECM, but the most common is collagen, which provides the ECM with several of its mechanical properties (Badylak, 2007). There are twenty eight known members of collagen, with collagen type I being the most common, but collagen type III is also found in large quantities in different tissue (Lieber, 2011). Fibrous proteins are the main structural element in the ECM, but are also involved in cell-ECM interaction, and regulating cell behavior. Understanding how the structure and composition of the ECM dictates normal tissue formation is essential for the creation of materials that may mimic its role during tissue engineering (Badylak, 2007). ECM is dynamic and its composition changes during development, this is visible from the several modifications that are made through the lifetime of the ECM from first forming during embryonic development to late adult life (Frantz et al., 2010).

1.6.1: Proteoglycans

Proteoglycans consist of a core protein with varying numbers of the same or different types of glycosaminoglycan (GAG) attached to the core protein through covalent binding, with the exception of hyaluronan (HA) that lack the core protein (Theocharis, Skandalis, Gialeli, & Karamanos, 2016). These GAG chains consist of negatively charged polysaccharides, which are made up of repeating unites of disaccharides (Frantz et al., 2010). There are two classes of GAGs based on the presence of sulfate (CS, DS, KS, and HS) or no sulfate (HA) (Schaefer & Schaefer, 2010). PGs are classified into three different groups based on their structure, composition, locations and functions. These different groups are the small leucine-rich proteoglycans (SLRPs), modular proteoglycans and cell-surface proteoglycans. The great diversity of PGs reflects the waste amount of different functions that PGs have in the ECM, such as cell signaling, proliferation and differentiation (Frantz et al., 2010; Theocharis et al., 2016). In the ECM the extracellular intestinal space is filled with PGs in the form of hydrated gel, providing the ECM with both flexibility and strength (Theocharis et al., 2016). Two important PGs in the ECM is decorin and biglycan, which both consist of a single core protein and one (decorin) or two (biglycan) sulfate side-chains, both belong to the class I of small leucine rich proteoglycans (SLRP) having around 10 leucine-rich repeats (Casar, McKechnie, Fallon, Young, & Brandan, 2004; Riessen et al., 1994). The two PGs affect the organization of the ECM by interacting with collagen and different matrix proteins to create the known fibrous network structure of the ECM (Casar et al., 2004). Decorin is expressed during differentiation while biglycan is expressed during myotube formation *in vivo* (Casar et al.,

2004). However, it has been shown that the expression of decorin and biglycan differ *in vitro*, with the expression of biglycan being most prominent during myoblast proliferation, and decorin being up-regulated in myotubes (Casar et al., 2004) .

1.6.2: Collagen

Collagen is the most abundant protein found in human cells, and is the main network forming protein in the ECM with 28 known types of collagen making up an estimated 30% of the total protein mass in a human (Theocharis et al., 2016). Collagens provides structural support and are essential for several different functions for different tissue and cells (Gordon & Hahn, 2010). Collagen is often secreted by fibroblast cells, which is recruited from nearby tissue, and influence the formation and organization of the collagen by applying pressure to the collagen fibers (Frantz et al., 2010). The main structural motif of collagen is that of three interconnected polypeptide α-chains, the α-chain pattern are gly-X-Y, with X and Y being different peptides, whereas the Y position is often taken by proline or hydroxproline (Gordon & Hahn, 2010). A total of forty six different α-chains; have been identified based on their polypeptide structure providing a vast complexity for different collagen (Theocharis et al., 2016). Collagen can be divided into two groups based on their fibril forming abilities, non-fibrillary and fibrillary collagens.

Fibrillar collagens are common structural support and load bearing proteins that are often found in tissue as a part of the ECM, and in this group one can find collagen type I, II, III, V, XI, XXIV and XXVII, which forms an interconnected fibrous network throughout the tissue (Theocharis et al., 2016). In tissue there is often one type of collagen that dominates, and with the wide difference in ECM composition across different types of tissues and developmental stages, the overall compositional difference for collagen can vary greatly from type of tissue to another, and from one developmental stage to another (Frantz et al., 2010).There is also a great difference in between the individual collagen fibers in both length and diameter, often reflecting the different roles and functions that the fiber plays in the tissue (Theocharis et al., 2016) Fibrous collagens assist in several different processes like cell adhesion, repair, regeneration, migration, proliferation and differentiation and is essential for the correct formation of tissue during development and repair (Frantz et al., 2010; Theocharis et al., 2016). Different types of collagen serve different roles in the ESM, collagen type III have been shown to maintain the function of several organs such as skin, but is also an essential component of the repair and regeneration system (Ohto-Fujita et al., 2011). The fibrous network of collagen that is spread throughout the tissue will often interact with other fiber

forming proteins in, which together forms the complex interconnected network that is tissue (Theocharis et al., 2016)

Inter-fibrillar collagens are structural proteins which are essential for forming the 3D structures in tissue, with inter-fibrillar collagens consisting of a triple helical motif similar to the common structural motif of other collagens, providing structures such as the ECM with flexibility, and interaction with other ECM components creating complex networks of different components (Theocharis et al., 2016). There are four collagens belonging to this class these are type IV, VI, VIII and X (Gordon & Hahn, 2010).

1.6.3: Fibronectin

Fibronectin (FN) is a fibrous protein that guides the organization of the ECM and meditates different cellular functions and cell adherences to the ECM (Frantz et al., 2010). FN is secreted by different fibroblast and myoblast cells during ECM formation, and is secreted as a polypeptide dimer hold together by disulfide bonds (Frantz et al., 2010). The structural motif of a single polypeptide monomer consist of three different modules, arranged in such a way that it binds proteins along its length (Sah & Rath, 2016).The FN dimer is able to bind to different structural components in the ECM such as collagen and other FN dimers making it possible for the FN dimer to form into long fibrils (Frantz et al., 2010). FN goes through several modifications such as alternative splicing which makes it possible for several different variants to exist, even if FN is only encoded by a single gene (Theocharis et al., 2016).

1.6.5: Elastin

Elastin is an amorphous protein characterized by its elasticity, and provides the ECM with flexibility through its interaction with different components like collagen, forming fiber networks that can provide recoil to different types of tissue (Rosso, Giordano, Barbarisi, & Barbarisi, 2004). Elastin is a major component of the tissue of the capillary system, lungs, hearts and muscles, which are types of tissue that often undergo stretching when in use and can be damaged if not able to withstand force pressure (Theocharis et al., 2016). The structure of elastin consist of two distinct parts: a cross-linked tropoelastin polymer which is assembled into fibers, and the microfibrils which assist in the cross linking of elastin (Frantz et al., 2010; Theocharis et al., 2016) Elastin have been linked to different diseases and overproduction of elastin in blood vessels can lead to the development of atherosclerosis (Theocharis et al., 2016)

1.7: The Eggshell membrane

The ESM have for the most part been overlooked by modern society due to being considered a waste product, however this is changing with more research and development being put into applications of the ESM, particularly in the field of medical science and the cosmetic industry which have produced products for the open marked (Sah & Rath, 2016). The ESM have shown potential in medical applications, particularly in fields related to treatment of burn and wound healing as several of the components of the ESM are also important in the repair system of the body (Vuong et al., 2017). In north eastern Asia, ESM have been used in holistic medicine for more than 400 years to treat burn wounds, and as a primitive bandage for wound healing (Vuong et al., 2017). The ESM has shown potential as a possible biomaterial for tissue engineering, due to it sharing several similarities with the ECM. The ESM and the ECM are similar in that both materials provides structural support, direct growth and protection from unwanted bacterial contaminations (Sah & Rath, 2016). There are also several physical similarities between the ESM and the ECM in architecture, such as the fibrous network, which consist of several of the same proteins like collagen, proteoglycans and different types of glycoproteins.

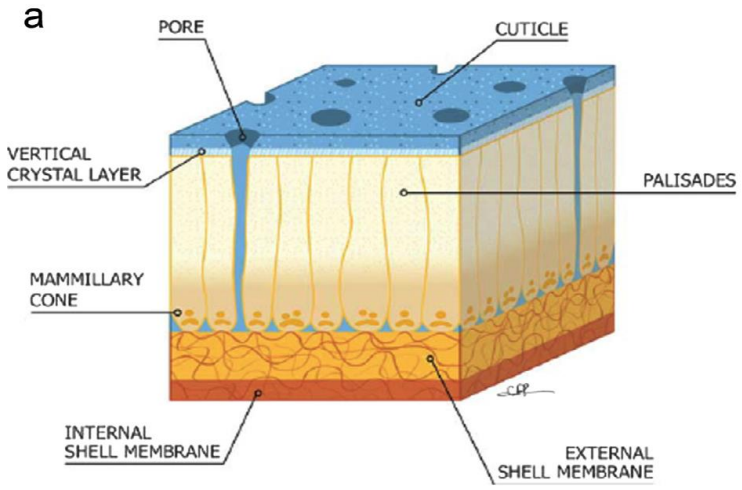

Figure 1.7A: Structure of the Eggshell membrane. *An overview of the different eggshell membrane parts, with the inner ESM membrane (Internal shell membrane) and outer ESM membrane (External shell membrane) in comparison to the eggshell (Palisades, vertical crystal layer and cuticle) inside the egg. Figure was reproduced from (Baláž, 2014) but originally published in (Lee et al., 2009).*

The eggshell membrane (ESM) is located between the inner surface of the eggshell and the egg white, and can be divided into two distinct parts: the inner and outer membrane (figure 1.7) (Tsai et al., 2006). The outer membrane is separated from the inner membrane by a layer of air, which is at its greatest distance in the air cell of the egg (Baláž, 2014). The outer

membrane is also partially integrated into the eggshell which makes it difficult to separate from the eggshell (Baláž, 2014). The outer and inner membrane differ in both architecture and composition, with certain types of collagen being more prominent in the outer membrane, and other types of collagens in the inner membrane; there is also a small variance in composition between the two membranes (Baláž, 2014). The fiber thickness between the outer and inner membrane differ: fibers of the outer membrane is between 1-7 lm in diameter, and the fibers of the inner membrane being between 0.1-3 lm in diameter (Baláž, 2014). The fibers of the two membranes are randomly orientated but the overall network is arranged parallel with the surface of the eggshell; each individual fiber is separated from each other by an internal space that is often filled with other ESM components (Baláž, 2014). The structure of the fibers in the inner membrane is more compact and smoother compared to the fibers of the outer membrane (Baláž, 2014). The total thickness of the outer ESM is between 50-70 µm, the inner membrane thickness is between 15-26 µm, and the total thickness of the two membranes is around 70 lm (Sah & Rath, 2016). The ESM consist of several different components such as collagen (type I, III and X), glycosaminoglycan (GAG), cysteine-rich eggshell membrane proteins (CREMPS) and hyaluronic acid (HA) which are all part of the fibrous network (Baláž, 2014). The structural composition of the ESM can be divided into two distinct groups; the organic (80-85%), which consists mainly of proteins, with collagen type I, V and X making up around 10% , and the inorganic (20-15%) which consist mainly of $CaCO_3$ (Baláž, 2014; Sah & Rath, 2016). The ratio between collagen I and collagen V is estimated to be around 100:1 for both membranes, with collagen type I found mostly in the outer membrane while the inner membrane contain collagen type I and V (Baláž, 2014). The ESM shares many similarities with the ECM, both are fibrous structure that contain collagen, hyaluronic acid (HA) and glycosaminoglycan (GAG), which have been related to wound healing and inflammatory regulation, and both materials are essential for structural support, signaling and antibacterial protection (Vuong et al., 2017). Hen egg white glycoprotein also present in the ESM and have been proven to show anti-inflammatory characteristics, which could be useful as the possibility to regulate inflammation during tissue regeneration is an important tool (Vuong et al., 2017). The ESM assists in several different processes inside of the egg, such as the formation of the eggshell during egg development and the removal of waste products through pores and protection against bacterial infections (Baláž, 2014). However, it should be noticed that the composition of collagen in the ESM have been regulated by changing the diet of the hens (Baláž, 2014).

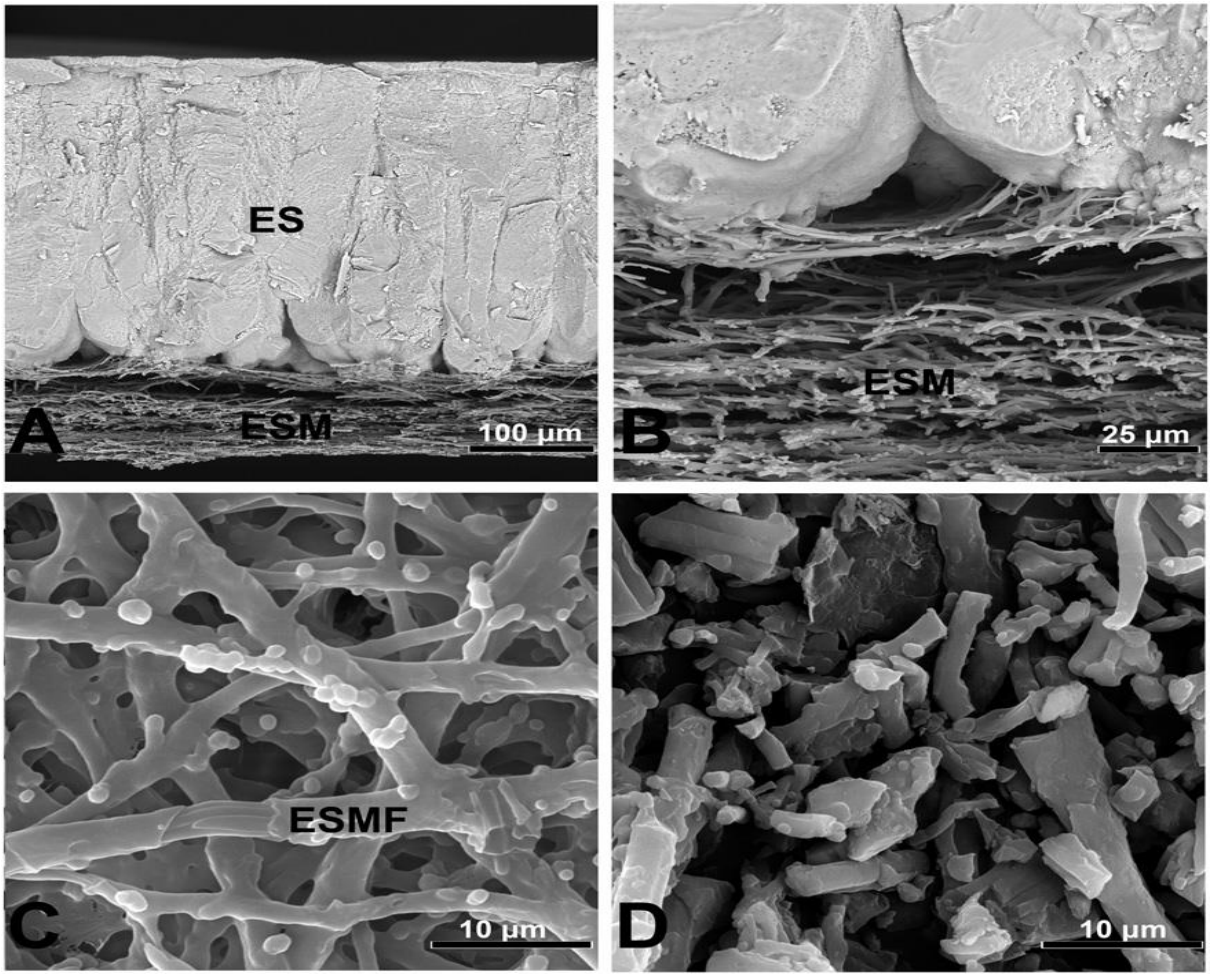

Figure 1.7B: SEM images of the eggshell and the eggshell membrane. *A) The difference in size between the inner and outer ESM and the ES. B) Close up of the ESM and ES area of interaction. C) Structural organization of the Eggshell membrane fibers (ESMF). D) Processed ESM, showing the fragmentation of the membrane structure into smaller components. Figure was reproduced from (Ahmed, Suso, & Hincke, 2017).*

2: Aim of the study

ESM has been shown to share several similarities with the ECM in composition and structural architecture, and it has been hypothesized that the ESM could provide a similar role in tissue formation as the ECM does *in vivo*. The ESM consist of several different components such as collagen, glycosaminoglycan and hyaluronic acid, which are also central components of the ECM, and have been linked to tissue formation and wound healing (Baláž, 2014; Frantz et al., 2010). Studies conducted at Nofima have also shown that ESM contain anti-inflammatory abilities, as well as promoting proliferation, differentiation and fibroblast migration (Vuong et al., 2017).

The aim of this study was to observe whether ESM at varying concentrations affects myoblast proliferation and differentiation, including the production and secretion of ECM components. Powdered and hydrolyzed ESM was tested in this study, with material obtained from industrial separated ESM. The effects of ESM materials on proliferation, viability and LDH-release were first tested, to identify optimal amount of ESM for the myoblast cells. The optimal amount was then used to study the effects of ESM on myoblast differentiation and ECM production by gene expression markers using real time-PCR. A further aim was to decide if ESM is a functional biomaterial in 3D scaffolding for muscle tissue generation. Scaffolds containing a mixture of collagen and ESM were compared to pure collagen scaffolds. The effects of the ESM-scaffold on myoblast proliferation and differentiation were visualized using immuno-staining, and changes in gene expression were evaluated using RT-PCR.

This thesis has been divided into two primary parts:

Part one: The effects of different ESM material in 2D environments on myoblast cells during proliferation and differentiation.

Part two: The effects of ESM scaffold on myoblast cells in a 3D environment during proliferation and differentiation.

3: Material

3.1: Kits

Name of Kit	Components	Producer
RNeasy mini kit(50)	RNeasy Mini Spin Columns(pink) Collection Tubes(1,5ml) Collection Tubes (2ml) Buffer RLT Buffer RW1 Buffer RPE RNase-Free Water Quick start protocol	Qiagen
RNase-Free DNase set (50)	Anhydrous D-glucose $CaCl_2x2H_2O$ $MgCl_2x6H_2O$ KCl Tris	Qiagen
Cytotoxic detection kit(LDH)	Dye solution Catalyst	Sigma-Aldrich
CellTiter-Glo® Luminiscent Cell Viability Assay	CellTiter-Glo® Buffer CellTiter-Glo® Substrate	Promega
CyQaunt® Proliferation Assay Kit	CyQuant GR Dye (Comp A) 1:400 Lysis buffer (Comp B) 1:20	Invitrogen
Taqman® RT-PCR kit	Deoxy NTP's Hexamer $MgCl_2$ 25mM Multiscribe RNase inhibitor 10x RT buffer	Applied Biosystems

3.2: Chemicals

Name of product	Producer/Supplier
10x Blocking buffer	Abcam
Dulbecco's Modified Eagle Medium Glutamax(+)	Thermo Fisher Scientific
Dulbecco's Phosphate Buffer Saline $CaCL_2$(-) $MgCl_2$(-)	Thermo Fisher Scientific
ECL Cell Attachment Matrix	Merck
Dimethyl Sulfoxide (DMSO)	Sigma Aldrich
Trypan Blue stain	Invitrogen
Trypsin	Thermo Fisher Scientific
Triton™ 100X	Sigma Aldrich
Fetal Bovine Serum	Sigma Aldrich
Tween® 20	Sigma Aldrich
Taqman® gene expression master mix	Applied Biosystems

3.3: Equipment

Product name	Producer/Supplier
Accurpette	VWR
Biopsy Punch	Kai medical
Blotting Roller	Invitrogen
Cell flask T75	Sarstedt
Cell culture multiflask TC,3-layer 525cm^2	Falcon
Countess™ cell counting chamber slides	Invitrogen
Cryotubes™ vials	Thermo scientific
Dako hydrophobic Pen	Dako Agilent
Eppendorf tubes (1,5ml)	Eppendorf
FinnPipette F2	Thermo scientific
Flat 8 cap strips	Thermo scientific
Nitrile powderfree disposable gloves XL	VWR
NuPage™ 10% Bis-Tris gel	Invitrogen
M.I.S.T magnetic Immuno Staining tray	Cell Path
Multiply®-µStrip 0.2ml chain	Sarstedt
Mounting medium fluorescence	Dako
Parafilm	Parafilm
Pipette tips(10, 50, 200 and 1000µl)	Sarstedt
Pipettes	Thermo scientific and BioHit
PCR plate (96-wells) half skirt	Sarstedt
QIA shredder mini spin columns	Qiagen
Surgical blade, Stainless steel	Swann morton
Serological pipettes (2.5, 5,10 and 25 ml)	Sarstedt and VWR
Sealing tape (96-well PCR plates)	Sarstadt
Sarstedt Tubes(15 and 50 ml)	Sarstedt
Tissue cell culture plates (White/black/Transparent), 96-wells	Thermo Scientific Nuncoln™ and Falcon
Hard tissue homogenizing CK28	Precellys

3.4: Medium for cell cultivation

Medium	Ingredients	Producer/Supplier
Proliferation	DMEM w/GLUTAMAX-I 2 % Foetal Calf Serum 2 % Ultroser G 0.5 % Pen/Strep 10.000 units/ml 0.5 % Fungizone (250µg/ml amphotericin)	Thermo Fisher Scientific
Differentiation	DMEM w/GLUTAMAX-I 2 % Foetal Calf Serum 0.5 % Pen/Strep(10.000 units) 0.5 % Fungizone(250µg/ml amphotericin) 25 µmol insulin	Thermo Fisher Scientific
Collagenase medium	DMEM medium 0.5 % Pen/Strep 0.5 % Fungizone 0,7 mg/ml Collagenase	Thermo Fisher Scientific
Seeding medium	DMEM w/GLUTAMAX-I 10 % FBS 0.5% Pen/Strep 2.5% Fungizone	Thermo Fisher Scientific
Medium used for cell storage in nitrogen	20% Proliferation medium 40% FBS 40% DSMO (20% dilution)	Thermo Fisher Scientific and Sigma Aldrich

3.5: RT-PCR Primers and Probes

Primer/probes	Product number	Producer/Supplier
EEF1A1	Bt03223794_g1	Applied BioSystems
TBP	Bt03241946_m1	Applied BioSystems
MYOD1	Bt03244740_m1	Applied BioSystems
MYOG	Bt03258928_m1	Applied BioSystems
Col1A1	Bt03225329_g1	Applied BioSystems
DCN	Bt03230910_m1	Applied BioSystems
BGN	Bt03244534_g1	Applied BioSystems

3.6: Instrument

Name of product	Producer/Supplier
Countess™ automated cell counter	Invitrogen™
Vacusafe	Integra
Centrifuge 5430	Eppendorf
SW22 Shaking water bath	Julabo
New Brunswick™ Galaxy 170S/R incubation locker	New Brunswick
VWR digital heat block	VWR®
LABXPert™	BRADY
Microcentrifuge MiniStar	VWR®
TX4 Digital Vortex Mixer with IR Sensor	VELP® Scientifica
See-Saw rockers-SSM4	Stuart®
Lab pH meter inoLab® pH7110	WTW
Hotplate stirrers, digital	Stuart®
PG204 DeltaRange®	Mettler Toledo
Precellys Evolution Homogenizer	Precellus
Microcentrifuges, ventilated/refrigerated Micro Star 17/17R	VWR®
LAF-bench:biohazard safety cabinet class 2	Scanlaf
Nanodrop®ND-1000 Spectrophotometer	Thermo scientific
GeneAMP®PCR system 9700	Thermo scientific
QuantStudio 5 Real-Time PCR System	Thermo scientific
Microscope Axio observer Z1	Zeiss
Microscope Leica DMIL LED	Leica microsystems
Canon EOS 550D	Canon inc
Leica CM3050 S Research Cryostat	Leica

3.7: Software

Name of product	Producer/Supplier
ImageJ 1.51w	Wayne Rasband
Zeiss ZEN blue edition	Carl Zeiss Microscopy
QuantStudio™ Design & Analysis Software	Thermo scientific
Microsoft Office Excel	Microsoft
Nanodrop ND-100 V3.81	Thermo Scientific

3.8: Primary Antibodies for immuno-staining

Name	Target Species	Mixing Ratio	Producer/provider
KI67	Rabbit	1:50	Abcam
NCAM	Mouse	1:10	The development studies hybridoma bank
WGA-594	Charged str.	1:300	Molecular Probes
Dapi Hochest-blue	Unspecified	1:1000	Molecular Probes

3.9: Secondary antibodies for immuno-staining

Fluorescent	Light(nm)	Target Species	Mixing Ratio	Producer/provider
Conjugated Dylight 549	549 nm	Anti-Goat	1:200	Abcam
Conjugated Alexa 488	488 nm	Anti-Rabbit	1:400	Thermo Fisher Scientific
Conjugated Dylight 549	549 nm	Anti-Mouse	1:400	Abcam

3.10: Buffers and solutions

Buffer/Solution	Reagents
TBS 10x(Tris buffered saline)	0.2 M Trizma Base 1.5M NaCl dH_2O pH at 7.6 with HCI 6N
TBS-Tween 1x	1:10 TBS 10x dH_2O 1:1.000 Tween 20

3.11: Scaffold

Name of scaffold	Composition	Producer/Supplier
Biovotec Control	0.75% Collagen	Biovotec AS, Dublin
Biovotec ESM	0.75% Collagen 3 % ESM	Biovotec AS, Dublin

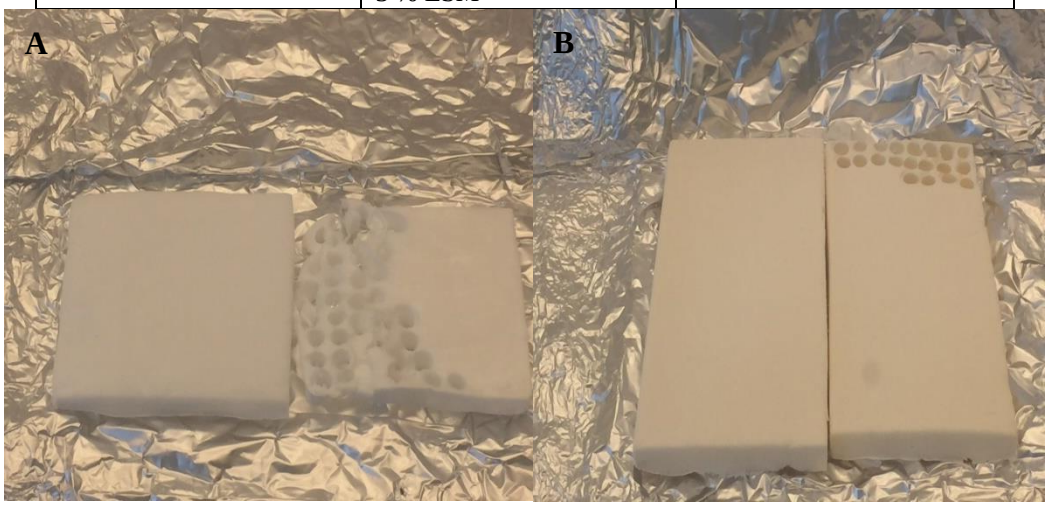

Figure 3.11: The primary scaffold pieces. *Smaller components were extracted from the primary structure of either the collagen scaffold (A) or the ESM scaffold (B).*

3:12: Additional

Name	Supplier
Freshly slaughtered sirloin from bovine	Nortura
Powdered ESM (ESM) Size: <100µm	Nortura,processed by Biovotec AS, Dublin.
Hydrolyzed ESM	Created at the company Nofima using ESM from Nortura

4: Methods

4.1: Origin of the eggshell membranes.

The ESM was extracted from hen eggshell and processed by the Norwegian food company *Nortura.* The method for extraction and processing are patented by the company *Biovotec,* located in Oslo, Norway (pat.nr: WO 2015/058790 A1) (Vuong et al., 2017). The eggshells were acquired as waste product from food production, and reduced to a powdered form through a process of drying and grinding in order to create the ESM material used during this study (Vuong et al., 2017). The composition of the ESM is that of crosslinked fibers, consisting of proteins, lipids and carbohydrates (Ahmed et al., 2017). ESM has been proven to retain both the fiber-like structure and carbohydrate components that the unprocessed ESM contained (Vuong et al., 2017). The hydrolyzed ESM was created at the company Nofima, through enzymatic degradation of the powdered ESM material.

4.2: Tips and tricks when working with myoblast cells.

During this study, MSCs were isolated from samples of freshly slaughtered sirloin taken from bovine. Bovine MSCs were chosen due to being both evolutionary closer to humans, and that the entire genome has been sequenced, making it easier to related any findings toward medical applications in humans (Rønning et al., 2013). Muscle tissue was chemically broken down through several steps, which separated the MSC from the tissue. Fibroblasts were removed using an uncoated cell vessels, taking advantage of the MSC need for a matrix to adhere to (Syverud, Lee, VanDusen, & Larkin, 2014). There are several advantages of chemically isolating cells from tissue, as it allows for large quantities of MSC to be isolated at once, while still keeping the number of fibroblast cell to an minimum; it has been shown that fibroblast cells will compose around 10% of the total cell population when using this method (Rønning et al., 2013). An advantage of using myoblast cells when studying muscles is that they are undifferentiated muscle cells that are still able to proliferate, making it easier to obtained large cell populations if needed; it is also possible to observe certain morphological changes using a microscope due to the size of the cells (Rønning et al., 2013). Myoblast cells are myogenic committed cells that has yet to initiate differentiation to form muscle fibers, making them excellent to be used in a model system when studying muscle and muscle development, reducing the amount of bias that may occur from using more specialized cells, and also making it possible to study any effects *in vitro* during both proliferation and differentiation (Rønning et al., 2013). Cellular differentiation is partially regulated by cell

density, which can be initiated when a sample reach 80-90 % confluence (Rønning et al., 2013). An uneven distribution of cells could also initiate differentiation, as small clusters of tightly packed cells could reach the required density for the process to be initiate (Rønning et al., 2013). Since differentiation can be initiated by cell density, it is essential that both cell distribution and population size can be regulated; this was done by splitting the cell populations into sub-populations, and then reseeding the sub-populations back into separate pre-coated culture vessels. Primary cells can only be spilt a finite number of times; splitting a culture seems to affect the cells negatively, reflected in reduced proliferation and differentiation rates, cell deaths and slower migration rates. It was also possible to initiate differentiation using serum deprivation, due to the fact that cells would only proliferate as long as growth factors were available; when growth factors were removed, cells would exit the proliferation phase and enter into differentiation (Rønning et al., 2013).

4.3: Isolating myoblast cells from bovine cattle.

Primary muscle cells were isolated from freshly slaughtered bovine sirloin, provided by the company *Nortura*, located in Lillehammer, Norway. To reduce the risk of contamination, each experiment was conducted in a sterile environment that was routinely washed with EtOH 75% before and after usage; equipment was also sterilized if possible. Cells were chemically isolated by breaking down sample tissue through several rounds of enzymatic digestion and tissue remains were removed using centrifugation and filtration. The advantage of chemically isolating cells is that the method can be used to isolate a large population at once, with high sample purity. It had been observed in other studies that around 10% of the total isolated cell population consisted of fibroblast cells when chemically isolating myoblast cells (Syverud et al., 2014). The extraction process was divided into three parts: cell isolation, proliferation of cell populations and liquid nitrogen preservation of cell lines.

Materials

- Biopsy needles
- Trypsin
- T25 and T75 culture vessels
- DMEM
- Tubes
- Proliferation medium
- Sowing medium

- FBS
- Collagenase (powdered)
- Sirloin taken from bovine (freshly slaughtered)

Protocol:

- Cells were isolated from tissue samples (1-2g) extracted from freshly slaughtered sirloin from bovine; tissue samples were extracted using a biopsy needle.
- Tissue samples were enzymatic digested using a collagenase mixture, which required that the powdered collagenase was sterile filtered before usage (see material 3.4 for the composition of the collagenase mixture).
- Tissue samples were incubated for 60 min at 37^{o}C in a shaking water bath at 70 rpm. Afterwards the samples were centrifuged at 550 RCF for 10 sec and the supernatant was filtrated while being transferred to another tube.
- Pellet was re-suspended in 20 ml trypsin and incubated in a shaking water bath for 15 min at 37^{o}C at 70 rpm. Tubes were turned every fifth minute.
- Afterwards samples were centrifuged at 550 RCF for 10 sec, and the supernatant was filtrated while being transferred to another tube. The Centrifugation step was repeated to ensure that the supernatant was removed.
- The two last steps were repeated two more times
- After finishing the trypsin treatment; the supernatant from the samples was transferred to uncoated T-25 flasks; this was done to remove unwanted fibroblast cells.
- The uncoated T-25 flasks were put in an cell incubator at 37^{o}C for 60 min. Afterwards the supernatant was transferred to an coated T-25 flask and incubated for 48 hours at 37^{o}C

Cells were monitored daily during proliferating. The cells were transferred from the T-25 flasks to coated T-75 flask when the density reached an observable threshold for further proliferation. Cells were frozen in liquid nitrogen when the cell population reached a desirable level.

4.4: Long time storage of muscle cells using liquid nitrogen

Storing organic material over an extended period of time to avoid degradation or contamination of the material, without reducing the quality of the samples, is essential for long running experiments. Nitrogen freezing is one of the best methods available for long time storage of cells. Due to the effective freezing using nitrogen, sample can be stored effectively and can be used with almost the same quality as before the samples were frozen.

Material:

- DMSO
- Proliferation medium
- Tubes
- Nitrogen storage tubes
- FBS

Protocol:

- Cells were put in special freezing tubes that are designed for longtime nitrogen storage. A mixture of 0.5 ml proliferation medium, 1 ml fetal bovine serum and 1 ml of 20% DMSO was added to the cells.
- The sample was put in a -20^{o}C freezer for 2-3 hours before being transferred to a -80^{o}C freezer, where the samples were stored for 24 hours.
- After 24 hours, the samples were transferred to the nitrogen storage unit for longtime storage.

4.5: Thawing and preparation of muscle cells

Removing cells from longtime storage in liquid nitrogen requires proper treatment. Cells that are not thawed correctly could die or suffer reduced performance which would affect the quality of the experiments. Thawing of cells was done in a sterile environment to avoid contamination. Overall cell thawing is a stepwise process which makes it possible transferred cell to a culture vessel for further study.

Material:

- Proliferation medium
- Tubes
- Eppendorf tubes

Protocol:

Before samples were removed from liquid nitrogen storage, proliferation medium was heated to 37^{o}C using a shaking water bath.

- Samples were extracted from liquid nitrogen and transported to a sterile environment and reheated by administrating proliferation medium dropwise and pipetting the medium slowly up and down. This was also done to dilute the DMSO which is toxic to cells.
- Samples were centrifuged at 550 RCF for 5 minutes and the supernatant was removed. Cell pellet was re-suspended in proliferation medium, counted and transferred to the desired culture vessel.

4.6: Splitting cell cultures

To regulate the amount of cells in a culture vessel, cultures were split by using trypsin to disassociate cells from the ECL attachment matrix. Splitting was used to regulate cells density, which could initiate unwanted cell differentiation, or to extract parts of the cell population for experimentation.

Material:

- PBS
- Trypsin
- Proliferation medium
- Tubes

Protocol

- Medium was removed, and the culture vessel was washed twice with PBS, this ensured that all medium was removed, as if medium remained cells would not disassociate from the cell-adhesion matrix.
- Trypsin was added, and the sample was placed in a cell incubator for 10 minutes at 37^{o}C.
- To ensure that cells had disengaged from the surface, a microscope was used to observe the sample. Disassociated cells could be observed as floating round objects, while cells that were still anchored to the surface would be more branched in structure.

- Sample was centrifuged for 5 minutes at 550 RCF to separate cells from the medium containing trypsin. After centrifugation, the supernatant was removed.
- Cell pellet was re-suspended using proliferation medium and then the total cell population was estimated, and divided accordingly.

4.7: Analyzing the total amount of cells.

The amount of cells in a given sample was estimated using the countess® automated cell counter. The cell counter gave an estimate of the total number of cells in a sample as cell/ml concentration. The total amount of cells was then estimated by multiplying the concentration with the volume of the primary sample.

Material:

- Eppendorf tubes
- Trypan Blue
- Cell counter plate
- Automatic cell counter

Protocol

- 10 µl was extracted from the primary samples which contained an unknown amount of cells, and placed in a 1.5 ml Eppendorf tube.
- 10 µl of trypan blue was then added to the Eppendorf tube and mixed and carefully mixed, the total volume was 20 µl.
- 10 µl of the mix was transferred to a counting slide and inserted in the countess® cell counter.
- The number of cells in a sample was estimated by multiplying the volume of the primary samples to the estimated concentration of the automated cell counter.

4.8: Seeding material with cell attachment matrix

To ensure that myoblast cells would adhere to the surface of a culture vessel, the ECL (Entactin-Collagen-laminin) coating material was used to create an artificial attachement matrix that cells could interact with. It had previously been shown that myoblast cells required an attachment matrix to be able to adhere to the surface of the culture vessel; if no attachment matrix was presented to the cell, many cells would not perform. The addition of ECL also provide a replacement for the missing ECM, which is essential for normal cell behavior and function (Rønning et al., 2013). It has been shown in previous studies that the addition of ECL to a sample do not significantly impact myogenesis (Rønning et al., 2013). All culture vessels that were used during this study were coated with ECL (See table 4.1 for the amount of ECL for different culture vessel).

Table 4.8: Culture vessels: *The different culture vessels used and the corresponding amount of ECL and cells for each.*

Culture vessel(flask/well)	Surface area(cm^2)	Number of cells when seeding	Proliferation med.(ml)	ECL(µl)
6 Well plate	10 cm^2	50.000	4 ml	30 µl
24 Well plate	2 cm^2	20.000	0.5 ml	6 µl
96 Well plate	0.3 cm^2	3.000	0.1 ml	0.9 µl
T-75 Flask	75 cm^2	200.000	15 ml	75 µl
T-25 Flask	25 cm^2	50.000	5 ml	25 µl
3 Layer flask	525 cm^2	1.000.000	60 ml	525 µl

Material

- ECL coating material
- Culture vessel
- DMEM

Process

- ECL was stored at -20^{o}C and needed to be thawed before use. Thawing was done on ice and ECL was kept on ice until added to the culture vessels.
- Culture vessels were coated with ECL, amount of ECL use differ with the surface area of the culture vessel. Ordinary DMEM medium was added with the ECL to ensure that the ECL was evenly distributed across the surface(See table 3.1 for the amount of ECL needed for the different culture vessels used)
- Coating medium was allowed to adhere to the surface of the culture vessel over a period of 2 hours
- Cells and cell medium was then added to the culture vessel.

4.9: ESM material

Four different methods were tested during this study of how to effectively present different ESM materials to the cells. These methods were free, coated, hydrolyzed and a mixed ESM (figure 4.9A-D).

Free ESM consisted of ESM that had been preprocessed into a powdered form and diluted using proliferation medium. The material was introduced directly to the cells in a 2D environment. The addition of free ESM was done after cells had been introduced to the surface of the culture vessel.

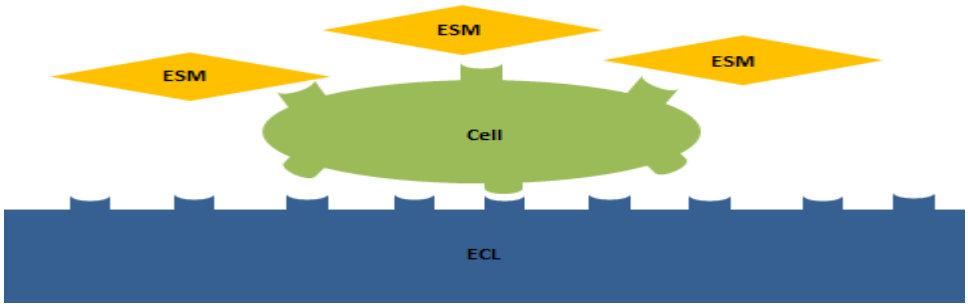

Figure 4.9A: Free ESM. *A schematic overview of how the ESM would interact with the cells in the culture vessel. ESM was added freely into the media, and the cells were seeded on ECL coated surface.*

Coated ESM was powdered ESM embedded into the ECL-coating surface. The mixture was added to the culture vessel and allowed to adhere to the surface over a period of 2-3 hours before the seeding of cells. The ECL would anchor the ESM to the surface of the culture vessel.

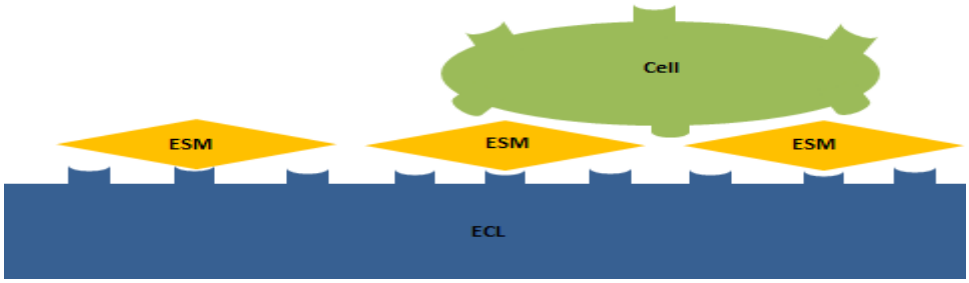

Figure 4.9B: Coated ESM. *A representation of how coated ESM would look like in the culture vessel. The ESM would be anchored to the surface of the culture vessel using the ECL attachment matrix.*

Hydrolyzed ESM material (Hydrol) was mixed with DMEM medium before it was added to the cell culture.

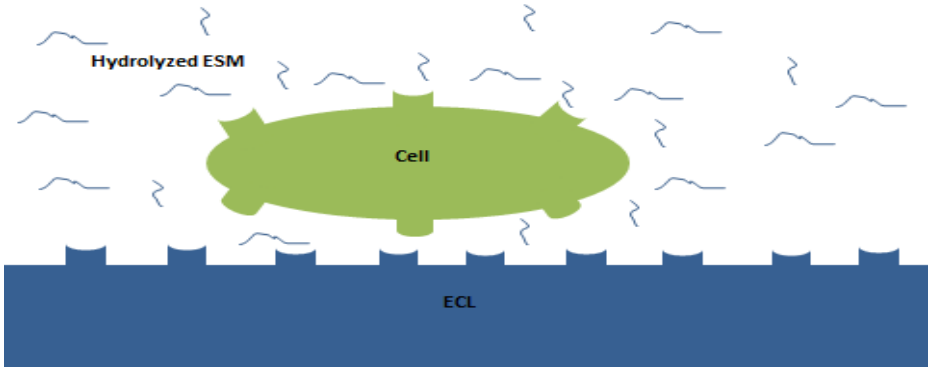

Figure 4.9C: Hydrol. *Hydrolyzed ESM was added to culture vessels that were coated with the ECL attachment matrix. Cells were added before the hydrolyzed ESM was added.*

Hydrolyzed and coated ESM mix (mixed) was created by first adding a coated ESM layer onto the surface of the culture vessel. Then the ESM was allowed to adhere to the surface of the culture vessel for a period of 2-3 hours. Hydrolyzed ESM was then added to the culture vessel without removing or damaging the coated ESM layer. Cells were added after ESM had adhered to the surface, but before the addition of hydrolyzed ESM.

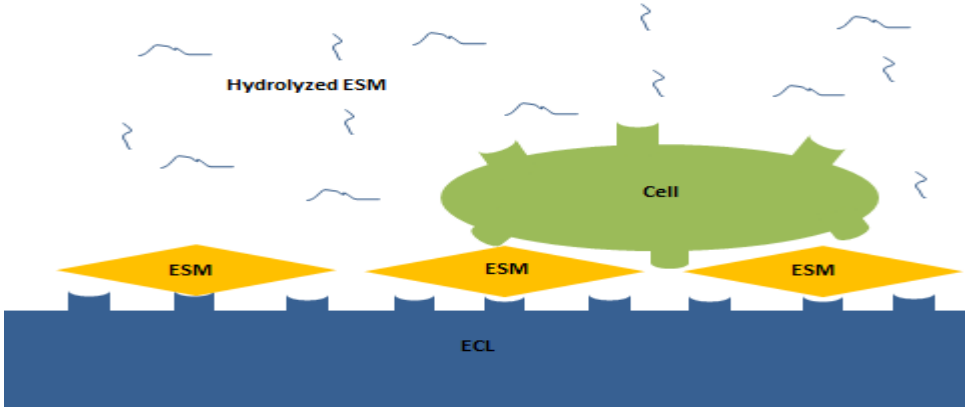

Figure 4.9D: Mixed ESM. *Mixed ESM was created by first introducing a coated ESM layer onto the surface of the culture vessel. Cells were added after the coated ESM had adhered, and then hydrolyzed ESM.*

4.10: The effect of ESM on muscle cell performance

4.10.1: Viability

The CellTiter-Glo®Luminiscent viability assay from Promega was used to estimate the viability for muscle cells proliferating on ESM or in hydrolyzed ESM. The assay takes advantage of extracted beetle luciferin, the enzyme luciferase, Mg^{2+} and O_2 to estimate the amount of ATP in a sample. When beetle luciferin, luciferase, Mg^{2+}, O_2 and ATP are all present; a light signal will be produced from the formation of oxylucuferin. The strength of this signal is proportional to the amount of ATP in the sample ("CellTiter-Glo Luminescent Cell Viability Assay," Last Revi. 2015).

$$Beetle\ Luciferin + ATP + O_2 \rightarrow Ultra\ Glo\ Recombinant\ Luciferase + Mg^{2+} \rightarrow Oxyluciferin + AMP + PP_i + CO_2 + \boldsymbol{Light}$$

The signal produced was detected using the Synergy H1 microplate reader twelve minutes after the addition of the viability assay to each sample.

Material

- Plate reader
- Tubes
- CellTiter-Glo® Luminiscent Cell Viability Assay
    - CellTiter-Glo® Buffer
    - CellTiter-Glo® Substrate

Protocol

- The CellTiter-Glo® assay kit was stored at -20°C. Components should be heated to around 20°C before use.
- 10 ml of CellTiter-Glo buffer was transferred to the CellTiter-Glo substrate, reagents were mixed using a vortex.
- Add the assay to each well, the amount added should be similar to the volume in each well, if 100µl sample, add 100µl assay for a total volume of 200µl. Keep samples in dark after the addition of assay.
- After adding assay to each well, put the plate on a shaker for about 2 minutes, and then wait 10 minutes before reading the fluorescent signal.

4.10.2: Proliferation

The CyQuant® Cell proliferation assay kit was used to estimate the effect of ESM and hydrolyzed ESM on muscle cell proliferation. The kit uses fluorescent lightning and DNA to estimate the amount of cells in a given sample. This is done by first freezing samples, improving the effect of the cell-lysis buffer which is added afterwards. If cells are successfully lysed, DNA will be released and can then interact with the fluorescent dye. The fluorescent light will correlates with the amount of DNA in the sample. It is then possible to calculate the increase in proliferation by comparing one sample with the control sample.

The signal produced was detected using the Synergy H1 microplate reader 10 minutes after the addition of the proliferation assay to each sample.

Material

- Plate reader
- CyQuant Proliferation assay Kit
    - CyQuant GR dye
    - Cell lysis buffer

Protocol

- Medium was removed from the wells and transferred to a new 96-well plate used for measuring cytotoxicity. After removing the medium, the plate was placed in a -80^{o}C freezer overnight.
- Lysis buffer was made following table 4.10.2

Table 4.10.2: Components for proliferation assay. *The given amount for each component represents a single well. All components were taken from the CyQuant cell proliferation kit.*

Components	Amount (µl)
Stock lysis	10.4
H_2O	200
Dye	0.525

- 200 µl lysis buffer was added to each well. Samples were then incubated without light for 10 minutes at around 20^{o}C before fluorescent was measured.

4.10.3: Cytotoxic

The cytotoxic detection kit from Sigma-Aldrich was used to estimate how cytotoxic the ESM material was to cells. The Cytotoxic detection kit interacts with lactate dehydrogenase (LDH) in the sample; LHD is released from cells due to damage to the plasma membrane and the amount of LDH can be used to estimate changes in cytotoxicity between samples and control (Roche, 2012) .

The signal produced was detected using the Synergy H1 microplate reader 30 minutes after the addition of the cytotoxic detection solution to each sample.

Material

- Cytotoxic detection kit (LDH)
    - Dye solution
    - Catalyst

Protocol

- Medium tested was taken from the proliferation test. Medium was transferred from a black 96-well proliferation plate to an empty transparent 96-well plate.
- Reaction mix was created following table 4.10.3 and added to each well, with the amount added equal to the amount of transferred medium. An example would be that if 100µl medium was transferred to the transparent 96-well plate, 100µl reaction mix would be added to each well.

Table 4.10.3: *The amount of reagents needed for a single cytotoxic sample. All ingredients were taken from the cytotoxic detection kit (LDH-release)*

Ingredients	Amount (µl)
Dye solution	2.5
Catalyst	112.5
Total	115

- Samples were left in a dark area for 30 minutes at room temperature before absorbance was measured.

4.11: Working with the 3D scaffolds

It was desirable to observe how muscle cells would interact with the ESM when presented in a 3D environment. The preference for using a 3D environments for tissue engineering, is that it more closely resemble the natural condition found during normal tissue formation, and therefore ensures that the new engineered tissue is more correctly formed (Ohto-Fujita et al., 2011). Two different types of scaffolds was tested: an ESM scaffold and a collagen scaffold that was designated as control. The control scaffold contained 0.75% collagen, while the ESM scaffold contained 0.75% collagen and 3% ESM. Both scaffolds were created by the company Biovotec AS.

Before cells were added to the 3D scaffold, it was necessary to separate smaller components from the primary scaffold (Figure 3.11); these smaller unites had to be disinfected before they could be used in further experiments. This method was used for both the ESM and collagen scaffold.

Material:

- EtOH (100% and 70%)
- Primary scaffold structure
- Scalpel
- Tweezer
- Biopsy Punch
- Proliferation medium
- 96 well plate
- PBS

Protocol:

- A scaffold component was separated from the primary scaffold piece, using a biopsy punch.
- The component was divided into slices (~2mm) using a tweezer and a scalpel to hold and cut the scaffold component. The slices were then distributed into separate wells on a 96-well plate.
- EtOH (100%) was added to each slice and kept in it for 30 minutes, it was important during this process that the EtOH did not dry up.
- EtOH (70%) was added to each slice, and kept in it for 30 minutes, it was important during this process that the EtOH did not dry up.
- EtOH was removed and proliferation medium was added, components were allowed to soak up the medium for 10 minutes before the medium was removed and new medium was added; this was done three times.

Addition of cells

- Old medium was removed, and proliferation medium with cells was added to each slice. The total number of cells for each slice was 4*10^5(400.000).
- Samples containing slices of the ESM and collagen scaffold with cells was incubated for desired timespan, with medium being changed every second day.

4.12: TaqMan Real-Time PCR

Taqman RT-PCR was used to examine gene expression molecular markers of myoblast proliferation and differentiation. The procedure is divided into two steps: reverse transcriptase step (RT-PCR) with synthesis of cDNA from RNA and a following amplification PCR steps with taqman probes. PCR runs cDNA through several phases of denaturation and annealing using the heat stable taqman polymerase to synthesize new DNA strands in-between (Schmittgen & Livak, 2008). The amount of cDNA in a sample is measured in real time, through the release of fluorescent dye during DNA synthesis. For the DNA polymerase to be able to synthesis new DNA, primers needed to anneal to the strands first; it is during this phase that the taqman probe also anneals. The taqman probe consists of three parts; a 3- end quencher, a 5-end fluorescent dye molecule and single stranded DNA sequence in-between that will anneal to a target sequence. During synthesis of dsDNA, the 5-end fluorescent dye will be cleaved off by the DNA polymerase 5-end nuclease activity, releasing it from the 3-end quencher. The release of the 5-end fluorescent dye from the quencher produces detectable light that can be measured. a single fluorescent dye is not strong enough to be detected, however as the PCR process amplifies the amount of DNA in the sample, more and more dye molecules will be released, creating a stronger signal ("Introduction to TaqMan® and SYBR® Green Chemistries for Real-Time PCR," last Rev 06/2010). The denaturation and aneling of dsDNA will run until the fluorescent signal is strong enough to be separate from the background noise in a sample. The number of runs needed to separate background noise from the sample is called ct-value, and it was used to calculate change in expression

4.12.1: Isolating RNA

RNA is easily degraded, and all samples had to be kept on ice when in use, or stored at -80^{o}C. Extraction of mRNA was done by adding RLT buffer to the cells, which destroys the cell membrane and allows the mRNA to spill out of the cell. The lysis process also releases unwanted gDNA and proteins, making sample purification necessary to ensure accurate data. The lysing process was done on 2D surfaces, by adding RLT lysis buffer directly to the surface. Lysis of cells living on 3D scaffolds was done by placing the scaffold and the lysis buffer into a homogenizer and physically breaking down the scaffold using beads to break the structure into pieces, allowing the lysis buffer to access the cells inside of the scaffold. Purifying samples containing remains from scaffolding proved difficult as the remains would clog the filters. Removing the residues through centrifugation and pipetting proved counterproductive, as the total amount of isolated mRNA decreased when the residues from scaffolding was removed before purification.

Sample purification is a stepwise process that removed any remaining residues by chemically breaking down undesired molecules such as DNA with DNase, and separating them from the sample by filtration, allowing the mRNA to remain in the sample. Material:

- NanoDrop ND-1000 spectrophotometer
- RNase-Free DNase set(50)
- RNeasy Mini Kit (50)
    - RLT-buffer
    - Collection tubes
    - RW1-Buffer
    - RPE-Buffer
    - RNase free water
- PBS
- EtOH 70%

Protocol:

Samples were always kept on ice, and all work was done in a sterile environment.

Lysis process

- Cells were washed with PBS twice to remove any medium.
- 350µl RLT lysis buffer were added to all samples. Scaffolds and RLT buffer was added together and taken through a homogenizer to break down the 3D structure of the scaffold. When all samples were lysed, they were either frozen down at -80^{o}C or taken directly to the purification process.

RNA purification

- DNase was prepared following table 4.12.1, DNase should be made ready before starting the purification process, store RNase on ice when not in use.

Table 4.12.1: DNase. *The amount presented is only for a single sample.*

Reagents	Amount (µl)
DNase Stock	10µl
RDD buffer	70µl
Total DNase user solution per sample	80µl

- 350µl EtOH was added to each sample for a total volume of 700µl. The entire volume of a single sample was transferred to a spin column containing a filter. Samples were centrifuging at 10.000 RPM for 15 sec. Elution was removed after centrifugation. This step was done twice when working with 3D scaffolds.
- 350µl RW1 buffer was added to each column, samples were centrifuged at 10.000 RPM for 15 seconds and elution was then removed afterwards.
- The DNase solution was added to each sample (80µl), samples air-dried for 15 minutes after the addition of DNase.

- 350µl RW1 buffer was added to each sample, columns were centrifuged at 10.000 RPM for 15 seconds. The elution was removed.
- 500µl RPE buffer was added to each column, and the centrifuged at 10.000 RPM for 15 seconds
- 500µl RPE buffer was added to each column and then centrifuged at 10.000 RPM for 2 minutes
- Column was centrifuged at 10.000 RPM for 1 minute. The collection tube was replaced with a new collection tube.
- 30µl RNase free water was added to each filter. Samples were centrifuged at 10.000 RPM for 1 minute. The RNase free water was returned to the filter and samples were centrifuged at 10.000 RPM again for 1 minute.
- 10µl of the water is taken for measuring amount of RNA and purity. The remaining 20µl is frozen at -80^{o}C

4.12.2: Reverse transcriptase

Reverse transcriptase is the transcription of mRNA into cDNA by a reverse transcriptase polymerase. The process is similar to that of DNA synthesis, but uses single stranded RNA as template for a new dsDNA strand. Reverse transcriptase is an important part of RT-PCR as the taqman-probes system uses dsDNA to estimate the amount of mRNA in a sample.

Material:

- Taqman® RT-PCR kit
- GeneAmp PCR system 9700
- Taqman gene expression master mix
- QuantStudio 5 Real-Time PCR System

$$mRNA + Revers\ transcriptase = cDNA$$

- Since RNA is easily degradable all samples were kept on ice.
- The Taqman mix was made following table 4.12.2

Table 4.12.2: Taqman mix: *The taqman mixture was made using the following concentrations. The amount given is only for a single sample.*

Reagents	Amount
10xRT buffer	2µl
$MgCl_2$ (25mM)	4,4µl
Deoxy NTP's	4µl
Hexamer	1µl
RNase inhibitor	0.4µl
Multiscribe	0.5µl
Total	**12.3µl**

- Amount of RNA needed for RT-PCR was calculated, ensuring that there was uniformity between samples.
- Taqman reagents was added to each sample, with a total volume of 20µl. Samples were put through the process of reverse transcriptase.
    - Program run for RNA samples was set to: 10 min at 25^{o}C, 30 min at 48^{o}C, 5 min at 95^{o}C and 4^{o}C end-run.
- H_2O was added to cDNA samples so that samples were diluted to the desired concentrations.
- Samples were stored at -20^{o}C.

4.12.3: RT-PCR

- Thawing was done while samples were kept on ice.
- Primers and probes were prepared following table 3.5.3

Table 4.12.3: Master Mix for RT-PCR. *The amount of each reagent needed to produce RT-PCR measurements. The total volume represents a single sample reaction.*

Reagents	Amount (µl) per well
Taqman gene expression master mix	10 µl
Primer and probes	5 µl
dH_2O	1 µl
Total	16 µl

- cDNA and the PCR master mix was added together on a 96-well PCR plate with 16 µl PCR master mix and 4 µl cDNA added to each well, for a total volume of 20 µl in each well.
- The PCR-plate was centrifuged at 1000 RPM for 1 minute, before being placed in the QuantStudio 5 Real-Time PCR machine. The following settings were used:

Step 1: 50°C for 02:00 minutes
Step 2: 95°C for 10:00 minutes
Step 3: 95°C for 00:15 minutes 40x
Step 4: 60°C for 01:00 minute 40x

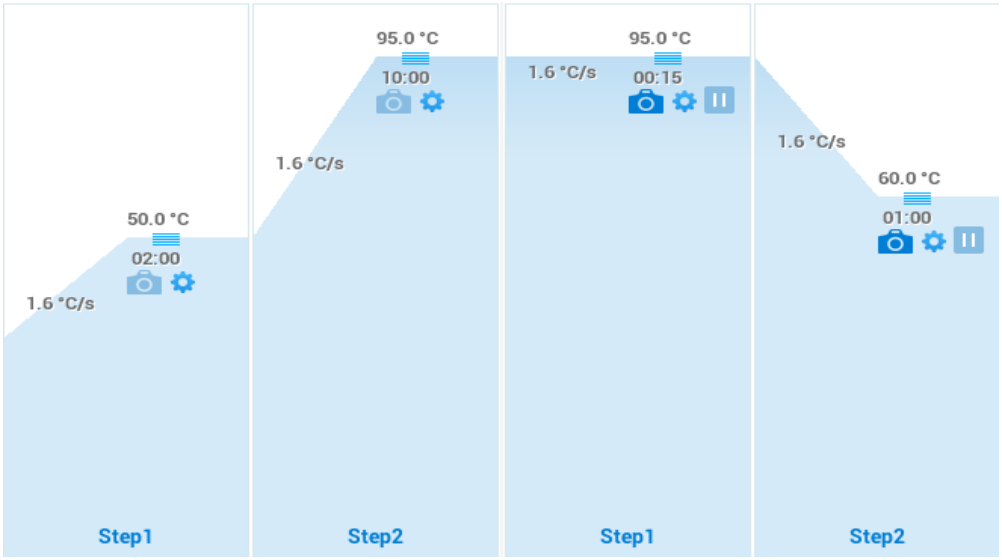

Figure 4.10.3: RT-PCR cycle. *The real time PCR cycle used for measuring gene expression for all samples.*

4.12.4: Calculating change in gene expression.

Change in expression was calculated by exporting ct-values from the RT-PCR process into excel and calculating fold change for each gene at different concentrations. Fold change is the change in expression for a particular gene compare to a reference gene. The given value in fold change equals an increase (>1.0), decrease (<1.0) or no change (1.0) in expression. A fold change value of 1.20 equals a 20% increase in expression compare to the control.

$$1: Ct_{gene} - Ct_{refrence-gen} = \Delta Ct$$

$$2: \Delta Ct_{treated\ samples} - \Delta Ct_{untreated\ sample} = \Delta\Delta Ct$$

$$3: 2^{-\Delta\Delta ct} = \text{Fold change}$$

Formula 4.12.4: Calculating fold change. *The formula used to calculate* ΔCt, $\Delta\Delta Ct$ *and fold change.*

4.13: Immunostaining of cells.

Immunostaining with fluorescently stained antibodies was first described by Albert H.Coons in his paper "The beginnings of immunofluorescent" is a well-used method for identifying different proteins (Coons, 1961). Immuno-staining takes advantage of antibody preference towards antigens to identify cellular components and structures. The process of immune-staining begins with fixation of the samples, which stops all cellular processes. Samples were either used directly or frozen at -80^{o}C. EtOH was used for cells on cover slides, while the liquid nitrogen was used for the 3D scaffold. Primary antibodies were introduced to the cells, to adhere to their target antigens. After the addition of primary antibodies, the secondary antibodies were added to the cells, these antibodies, containing a fluorescent dye molecule, attached themselves to the primary antibodies, making it possible to observe the different cellular components through a microscope. Experiments were divided into 2D immuno-staining of cells and immuno-staining of 3D scaffold structure.

Materials for 2D immuno-staining:

- 24-well plate
- Cover slides (round)
- EtOH (96%)
- PBS
- ECL
- Antibodies (primary and secondary)

Materials for 3D immuno-staining:

- Liquid nitrogen
- Microscope slides
- PBS
- Dako hydrophobic pen
- 10x blocking buffer
- Mounting medium
- Antibodies(primary and secondary)

Protocol:

Preparing of samples for immune-staining (2D only):

- Cover slides (round) were placed into wells using a tweezer, then was sterilized with EtOH (96%) for 15 min.
- EtOH was removed, and ECL coating matrix was added to the coverslides, and allowed to adhere in RT for 2-3 hours.
- Cells were added
    - 20.000cells /pr well on a 24 well plate.
    - 10.000cells /pr well on camper slides
- Cells were allowed to proliferate for 48 hours with proliferation medium.

Immuno-staining during 2D:

- Medium was removed from samples, and then washed twice with PBS.
- Fixation and permabilization of cells was done by adding cold (-20^{o}C) EtOH (96%) to the cells for 15 minutes in RT. Afterwards the samples were washed three times using PBS.
- Blocking was achieved using a 1:10 dilution a 10x blocking buffer for 30-60 minutes. Blocking buffer was diluted using PBS.
- Primary antibodies were diluted using the PBS-twee; then added to the samples for 30-60 minutes. Afterwards the samples were washed with PBS 3x10 minutes.
- Secondary antibodies were diluted with PBS-tween and added to the sample in a dark area for 30-60 minutes.
- Unnecessary liquid was removed by carefully washing the cover glass with dH_2O, and then drying the samples using a paper towel.
- When adding the cover glass, a drop of mounting medium was used to hold the glass in place. Air bobbles that formed while adding the cover glass was removed by pressing the air carefully out.
- Samples were observed through the microscope Axio observer Z1 from Zeiss.

Preparing samples for immuno-staining (3D only)

- Scaffolds were prepared following the protocol 4.11: working with the 3D scaffold.

Immuno-staining during 3D

- 3D scaffolds were prepared for immuno-staining using cryo-fixation with liquid nitrogen.
- Scaffolds were cut into layers that were then attached to a microscope slide, and stored at -20^{o}C.
- An area around the scaffolds were marked with the dako hydrophobic pen, this was done to ensure that sample did not run off.
- Blocking was achieved using a 1:10 dilution of the 10x blocking buffer for 30-60 minutes. The blocking buffer was diluted using BPS.
- Primary antibodies were diluted using the PBS-tween then added to the samples for 30-60 minutes. Afterwards the samples were washed with PBS 3x10 minutes.

- Secondary antibodies were diluted with PBS-tween and added to the sample in a dark area for 30-60 minutes.
- Unnecessary liquid was removed by carefully washing the cover glass with dH_2O, and then drying the samples using a paper towel.
- When adding the cover glass, a drop of mounting medium was used to hold the glass in place. Air bobbles that formed while adding the cover glass was removed by pressing the air carefully out.
- Samples were observed through the microscope Axio observer Z1 from Zeiss.

4.14: Cell migration assay.

The migration rate for cells was tested on a 2D surface with 0.01 mg/ml and 0.0001 mg/ml concentration of coated ESM. Cells were allowed to proliferate for 48 hours to ensure that an appropriate cell density was obtained on the surface before the migration rate was tested. After 48 hours, a pipet was used to scratch a small area to remove cells, forming a crosslike "wound or scratch" across the surface, which the cells could migrate into (Yarrow, Perlman, Westwood, & Mitchison, 2004). After the introduction of the wound, the migration rate was observed using a microscope over a 24 hour period.

Material

- 6 well plate
- Microscope
- ECL
- Proliferation medium
- Differentiation medium

Protocol

- The culture vessel was prepared, and cells were allowed to proliferate for 48 hours.
- Wound was introduced by scraping a pipet across the cell surface.
- Cells were then observed at five different points in time, and pictures were taken each time at 4x and 10x enhancement.
    - 0 hours after introducing the wound
    - 2 hours after introducing the wound

    - 4 hours after introducing the wound
    - 6 hours after introducing the wound
    - 24 hours after introducing the wound
- Change in migration was calculated by measuring the distance between the sides of the wounds using imageJ, and then comparing the distance to the control for any changes in migration rates.

5: Results

5.1: Successful extraction and identification of isolated muscle cells.

Muscle satellite cells were extracted from newly slaughtered sirloin taken from bovine through chemically breaking down muscle fibers using a stepwise process that separated the satellite cells from the muscle fibers. Breaking down fibers chemically made it possible to isolate a large amount of satellite cell with a small presents of fibroblast. In order to separate the satellite cells from unwanted fibroblast cells, the samples were put in an uncoated tissue flask that only the fibroblast would adhere to, as myoblast cells needs a matrix to attach to, the sample was then removed and fibroblast would remain attached to the tissue flask. Myoblast cells were then stained with different antibodies to identify cellular components. Immuno-staining with the known muscle marker neural cell adhesion (NCAM), which can be observed on the surface of the cell and KI67 is strongly associated with cell proliferation, and is primarily found inside the cell nucleus. These results (figure 5.1) demonstrated that isolated cells expressed NCAM, and were capable of proliferating, which makes the cells suitable for further experiments.

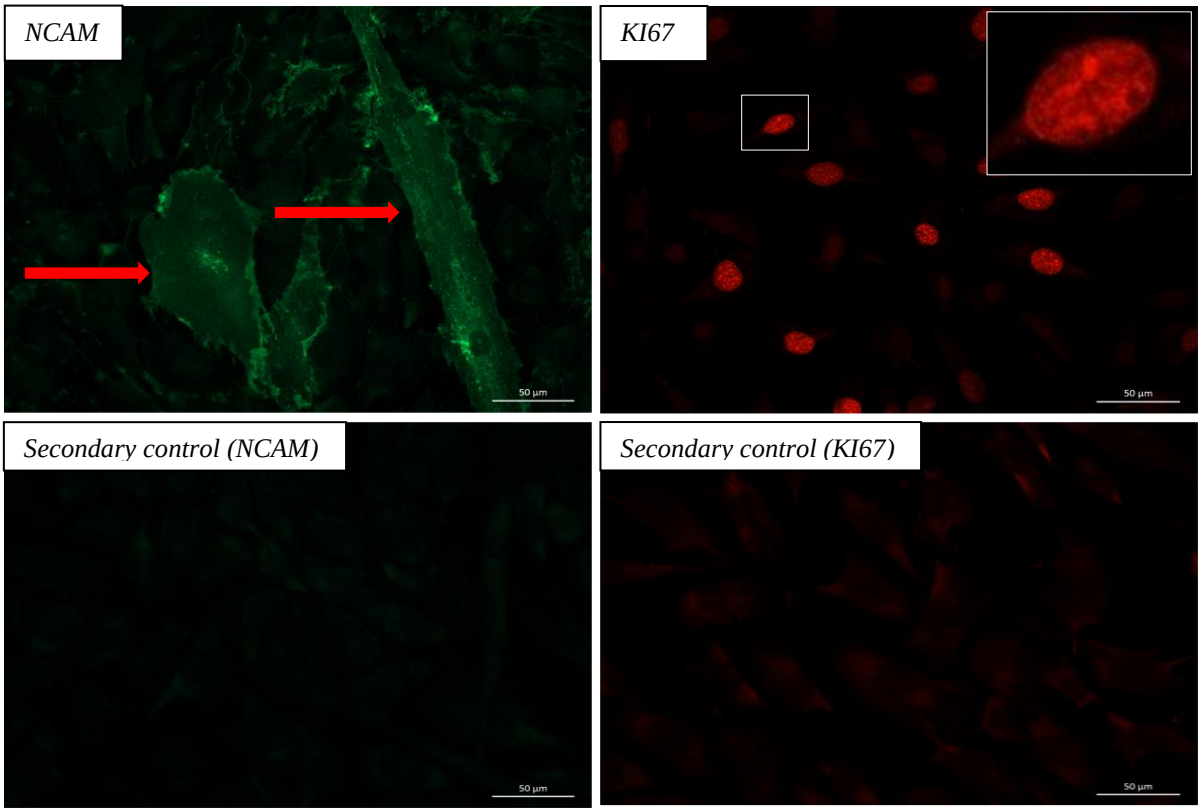

Figure 5.1: Identity and characteristics of muscle cells: *Cells were fixed using ice-cold EtOH, and then stained with primary antibodies, left image was stained with mouse (anti-NCAM) and right image was stained with rabbit (anti-KI67). Secondary antibodies were added, left image was stained with goat anti-mouse alexa 488 (green) and right with donkey anti-rabbit conjugated DyLight 649 (red). Samples were then observed and analysed using the ZEISS Axio Observer Z1 microscope. Red arrows indicate NCAM positive cells. Secondary control was only stained with secondary antibodies. The magnified area in KI67 shows a close up of a cell nucleus with the presence of Ki67 (red), which indicates that the cell is proliferating.*

5.2: The Effect of ESM material on muscle cells performance.

5.2.1: Negative impact of ESM material on muscle cell viability

A dose-response experiment, using five concentrations of both powdered and hydrolyzed ESM material was performed. The ESM material was presented to the cells in various ways as described in figs 4.9A-D. Cells were allowed to proliferate for 48 hours in the presence of ESM before viability was measured by fluorescence. Viability was estimated by the amount of fluorescent light emitted, which correlated to the amount of ATP present in the sample; this provide an approximation of the total number of metabolically active cells. The results (Table 5.2.1) showed a significant decrease in viability when the different ESM materials was presented to the cell compare to control, for the majority of samples. Cells cultivated on coated ESM at concentrations of 0.01mg/ml to 0.0001 mg/ml did not reduce viability. Control was set to 100% and samples were normalized against control. Overall the decrease in viability was reduced when cells were allowed to interact with decreasing amount of ESM.

Interestingly, this seems to indicate that, the way in which ESM is presented seems to matter to the cells, as coated ESM had no effect on viability compared to ESM that was presented freely to the cells. Overall, (figure 5.2.1) coating the powdered ESM material to the bottom of the surface of the culture well had a less negative impact on viability, with concentrations of 0.01-0.0001mgl/ml having no effects on viability.

Concentrations	Type	Test	Mean(%)	St.dev %
3 mg/ml	Free	Viability	73,67	17,71
1 mg/ml	Free	Viability	61,10	25,14
0.3 mg/ml	Free	Viability	54,13	20,76
0.1 mg/ml	Free	Viability	36,47	13,16
0.01 mg/ml	Free	Viability	72,75	22,95
0.001 mg/ml	Free	Viability	68,99	31,74
0.0001 mg/ml	Free	Viability	83,63	35,31
3 mg/ml	Coated	Viability	71,83	21,60
1 mg/ml	Coated	Viability	59,10	15,75
0.3 mg/ml	Coated	Viability	58,66	6,15
0.1 mg/ml	Coated	Viability	62,41	19,33
0.01 mg/ml	Coated	Viability	97,03	9,99
0.001 mg/ml	Coated	Viability	101,29	11,23
0.0001 mg/ml	Coated	Viability	104,46	11,53
5 mg/ml	Hydrolyzed	Viability	0,05	0,03
4 mg/ml	Hydrolyzed	Viability	0,07	0,02
3 mg/ml	Hydrolyzed	Viability	0,67	0,60
1 mg/ml	Hydrolyzed	Viability	25,21	18,45
0.3 mg/ml	Hydrolyzed	Viability	54,24	22,30
0.1 mg/ml	Hydrolyzed	Viability	42,06	8,10
0.01 mg/ml	Hydrolyzed	Viability	57,97	38,95
3 mg/ml	Hydrolyzed+ Coated	Viability	0,86	0,73
1 mg/ml	Hydrolyzed+ Coated	Viability	37,23	3,67
0.3 mg/ml	Hydrolyzed+ Coated	Viability	47,83	4,01
0.1 mg/ml	Hydrolyzed+ Coated	Viability	43,42	7,02
0.01 mg/ml	Hydrolyzed+ Coated	Viability	49,75	10,45
4/0.001 mg/ml*	Hydrolyzed+ Coated	Viability	0,32	0,41
5/0.0001 mg/ml**	Hydrolyzed+ Coated	Viability	0,13	0,09

Table 5.2.1: The effect of ESM on myoblast viability: *Gray values indicated no change (95-105) while red values indicates a decrease (95-) in overall viability. The value Mean (%) represents the mean value of samples with the same characteristics such as concentrations and ESM material. Percentage change in viability was calculated using the mean of control as 100% and normalized sample data against control. Standard deviation (St.dev %) was calculated for each individual Mean (%)-value. Cells proliferate on free, coated, hydrolysed and a mixed ESM for 48 hours before data was collected. All samples with the exception of coated ESM 0.01-0.0001 mg/ml showed a decrease in viability.* 4 mg/ml hydrolysed ESM on a 0.001 mg/ml coated ESM surface. ** 5 mg/ml hydrolysed ESM on a 0.0001 mg/ml coated ESM surface.*

5.2.2: ESM materials seems to inhibit muscle cell proliferation

Proliferation was estimated from the amount of DNA present in a sample through fluorescent light using the CyQuant®Cell proliferation kit. Muscle cells proliferated on 2D surfaces using a 96-well plate over a 48 hour period on different types of ESM material similar to the layout for estimation of viability. Measurements (Table 5.2.2) showed a reduction in proliferation compare to control for all samples expect one, which showed no significant change in proliferation. Data showed that the greatest decrease in proliferation was for cells living in samples that contained some form of hydrolyzed ESM. Cells on coated ESM had the smallest decrease in proliferation compared to control; this seems to indicate that cell proliferation is mostly affected by how ESM is presented to the cells, with free and hydrolyzed ESM showing the clearest decrease in proliferation.

Concentrations	Type	Test	Mean(%)	St.dev %
3 mg/ml	Free	Proliferation	59,38	15,07
1 mg/ml	Free	Proliferation	53,80	20,46
0.3 mg/ml	Free	Proliferation	49,25	21,85
0.1 mg/ml	Free	Proliferation	44,61	20,86
0.01 mg/ml	Free	Proliferation	52,12	24,10
0.001 mg/ml	Free	Proliferation	52,33	14,94
0.0001 mg/ml	Free	Proliferation	35,93	12,95
3 mg/ml	Coated	Proliferation	85,64	20,16
1 mg/ml	Coated	Proliferation	83,57	23,75
0.3 mg/ml	Coated	Proliferation	78,35	20,78
0.1 mg/ml	Coated	Proliferation	86,45	18,77
0.01 mg/ml	Coated	Proliferation	92,89	23,61
0.001 mg/ml	Coated	Proliferation	97,18	19,73
0.0001 mg/ml	Coated	Proliferation	85,49	10,60
5 mg/ml	Hydrolyzed	Proliferation	11,30	4,84
4 mg/ml	Hydrolyzed	Proliferation	12,62	3,76
3 mg/ml	Hydrolyzed	Proliferation	31,98	12,14
1 mg/ml	Hydrolyzed	Proliferation	55,71	13,47
0.3 mg/ml	Hydrolyzed	Proliferation	44,61	5,98
0.1 mg/ml	Hydrolyzed	Proliferation	38,08	15,75
0.01 mg/ml	Hydrolyzed	Proliferation	35,30	10,47
3 mg/ml	Hydrolyzed+ Coated	Proliferation	58,14	18,06
1 mg/ml	Hydrolyzed+ Coated	Proliferation	73,46	16,86
0.3 mg/ml	Hydrolyzed+ Coated	Proliferation	66,71	17,47
0.1 mg/ml	Hydrolyzed+ Coated	Proliferation	48,97	5,99
0.01 mg/ml	Hydrolyzed+ Coated	Proliferation	36,65	27,98
4/0.001 mg/ml*	Hydrolyzed+ Coated	Proliferation	12,22	4,83
5/0.0001 mg/ml**	Hydrolyzed+ Coated	Proliferation	10,57	3,33

Table 5.2.2: The effect of ESM material on proliferation: *Gray values indicated no change (95-105) while red values shows a decrease (<95) in proliferation. The value Mean (%) represents the average percentage value for samples with the same layout. Percentage change in proliferation was calculated by normalizing sample values against control. Standard deviation (St.dev %) was calculated for each individual Mean (%)-value with significant outliers being removed. Cells were allowed to proliferate on the tested ESM materials for 48 hours before measured and data was collected. Only cells on 0.001 mg/ml coated EMS was not significant affected by the introduction of ESM material, all other types of ESM material showed a reduction in proliferation. * 4 mg/ml hydrolysed ESM on a 0.001 mg/ml coated ESM surface. ** 5 mg/ml hydrolysed ESM on a 0.0001 mg/ml coated ESM surface.*

5.2.3: Coated ESM material is less cytotoxic to muscle cells.

The cytotoxic effect of ESM was estimated through a dose-responses experiment that measured change in absorbance as a result of LDH-release (lactate dehydrogenase), which happens due to the cell membrane being compromised ("Pierce LDH Cytotoxicity Assay Kit," last accessed 2018). The effect of different ESM materials on cytotoxicity was tested at concentrations ranging between 5-0.0001mg/ml over a period of 48 hours. The cytotoxic detection kit from Sigma-Aldrich was used to provide accurate results (see method 4.9.3). The results showed that ESM materials were cytotoxic for the majority of samples. However, low concentrations of coated ESM reduced cytotoxicity. The reduction in cytotoxicity for coated samples seems to correlate with similar results from the viability and proliferation tests, in that the way a material is presented affects cells activity. Hydrolysed ESM at 3 mg/ml was unaffected by the ESM material. The greatest increase in cytotoxicity was for cells interacting with free PEP.

Concentrations	Type	Test	Mean(%)	St.dev %
3 mg/ml	Free	Cytotoxic	151,27	35,88
1 mg/ml	Free	Cytotoxic	136,41	19,66
0.3 mg/ml	Free	Cytotoxic	149,42	19,37
0.1 mg/ml	Free	Cytotoxic	137,88	14,22
0.01 mg/ml	Free	Cytotoxic	121,50	12,59
0.001 mg/ml	Free	Cytotoxic	124,97	15,38
0.0001 mg/ml	Free	Cytotoxic	129,03	13,22
3 mg/ml	Coated	Cytotoxic	111,74	24,07
1 mg/ml	Coated	Cytotoxic	109,72	15,72
0.3 mg/ml	Coated	Cytotoxic	120,83	21,59
0.1 mg/ml	Coated	Cytotoxic	121,27	15,63
0.01 mg/ml	Coated	Cytotoxic	93,22	14,16
0.001 mg/ml	Coated	Cytotoxic	91,08	15,43
0.0001 mg/ml	Coated	Cytotoxic	90,33	16,71
5 mg/ml	Hydrolyzed	Cytotoxic	113,78	9,99
4 mg/ml	Hydrolyzed	Cytotoxic	102,29	24,63
3 mg/ml	Hydrolyzed	Cytotoxic	99,35	13,30
1 mg/ml	Hydrolyzed	Cytotoxic	107,99	20,06
0.3 mg/ml	Hydrolyzed	Cytotoxic	115,45	19,45
0.1 mg/ml	Hydrolyzed	Cytotoxic	123,64	17,42
0.01 mg/ml	Hydrolyzed	Cytotoxic	137,51	16,69
3 mg/ml	Hydrolyzed+ Coated	Cytotoxic	126,87	15,63
1 mg/ml	Hydrolyzed+ Coated	Cytotoxic	128,98	14,62
0.3 mg/ml	Hydrolyzed+ Coated	Cytotoxic	125,74	8,30
0.1 mg/ml	Hydrolyzed+ Coated	Cytotoxic	112,17	17,76
0.01 mg/ml	Hydrolyzed+ Coated	Cytotoxic	110,33	16,17
4/0.001 mg/ml*	Hydrolyzed+ Coated	Cytotoxic	112,89	17,12
5/0.0001 mg/ml*	Hydrolyzed+ Coated	Cytotoxic	117,59	16,86
2 % Trition-X***		Cytotoxic	476,57	25,35

Table 5.2.3: ESM materials effect on LDH release. *Gray values indicates no significant change (95-105) while red values indicates an increase (>105) and green values a decrease (<95) in LDH-release compare to control. The value Mean (%) represents the mean value for samples with similar characteristics. Percentage change in cytotoxicity was calculated using the mean of control (100) to normalizing sample data. Standard deviation (St.dev %) was calculated for each individual Mean (%)-value, and major outliers were removed. Cells proliferate on the different methods of presenting ESM material for 48 hours before data was collected and percentage change was calculated. Data showed a small decrease in LDH release for cells living on coated ESM for concentrations between 0.01 and 0.0001mg/ml. LDH release was unchanged compare to control for cells living in 4 and 3 mg/ml hydrolyzed ESM. Cytotoxicity levels increased for all other samples. * 4 mg/ml hydrolyzed ESM on a 0.001 mg/ml coated EMS surface. ** 5 mg/ml hydrolyzed ESM on a 0.0001 mg/ml coated ESM surface. *** 2% Trition-X is positive control for samples.*

5.3: The effect of ESM coating on cell phases.

Previous experiments showed that coated ESM had the most desirable effects on muscle cells performance at concentrations between 0.01-0.0001mg/ml. Further testing was conducted to study the effects of coated ESM over an extended period of time, during both the proliferation and differentiation phase. Culture vessels were first coated with ESM, which was allowed to adhere over a period of 3 hours; cells were added afterwards. Muscle cells were first kept on proliferation medium for 72 hours (3 days) before the medium was changed to the differentiation medium. After the medium change, cells were kept on the differentiation medium for another 72 hours (3 days) before being lysed. Cells were observed for a total of six days, with pictures being taken each day during the experiment. There was no visible effect between samples and control while cells were in the proliferation phase. During cell differentiation there was observed an visible increase in the number of differentiating cells compare to the control at day 4 and 5 for both coated samples (0.01 and 0.0001mg/ml). After six days on the differentiation medium, no more visible difference between the samples and control was observed.

	0 mg/ml	*0.01 mg/ml*	*0.0001mg/ml*
*Day 1**		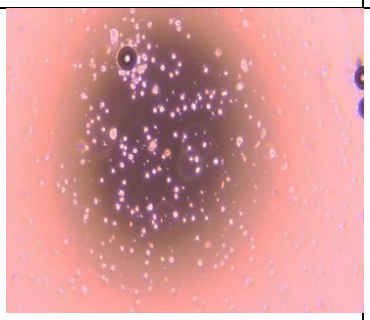	
Day 2	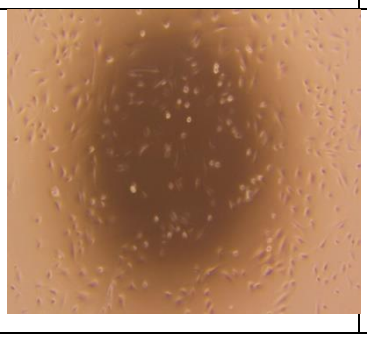	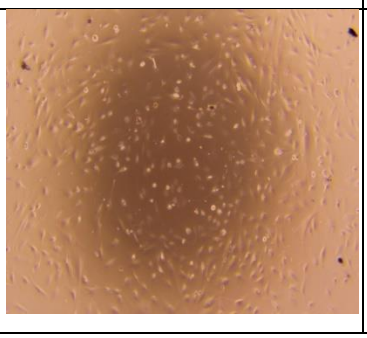	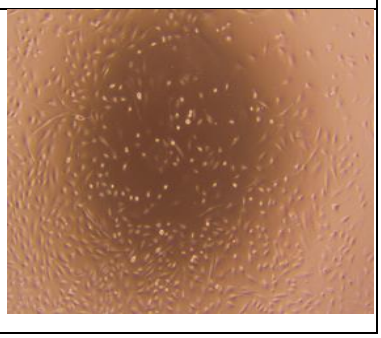

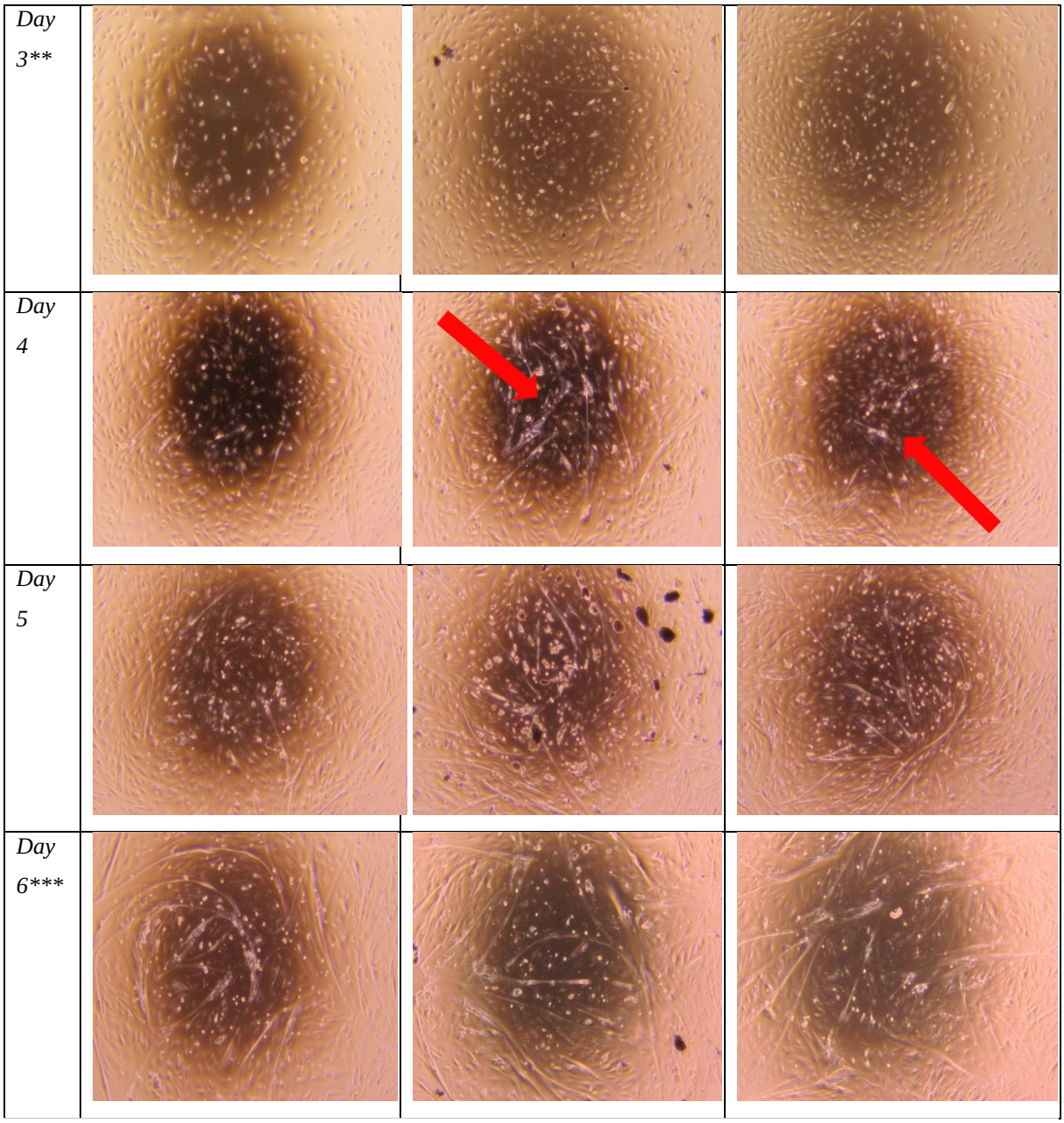

Figure 5.3: Different cellular stages for muscle cells at different concentrations of ESM. *Muscle cells were seeded on a 2D surface with coated ESM at two different concentrations over a period of six days. The cells were allowed to interact with proliferation medium for about three days (72 hours), before being replaced with differentiation medium. After six days all cells were lysed. The greatest change between cells was observed at day 4 and 5, the cells living in coated ESM showed clearer signs of differentiation than the cells in 0 mg/ml. * First stage, cells were in the process of adhering to the ECL coating material in the well. ** Proliferation medium was change to differentiation medium. *** Last day before cells were harvested. Red arrows indicate the presence of differentiated cells in sample.*

5.3.1: Cell migration on a 2D surface.

Cell migration was performed on 2D surfaces that were coated with ESM, at 0.01mg/ml and 0.0001 mg/ml concentrations. Migration was measured at 0 hours, right after the introduction of the wound, and was used at the control to calculate the migration speed for all concentrations after 2,4 and 6 hours. Samples were also measured at 24hours, however little to no sign remained of the "wound" and was therefore considered closed. Cell grown on ESM showed a decreased rate of migration in the beginning, however after six hours there was a tendens that cells living on coated ESM had increase migration rate compared to cells living without coated ESM.

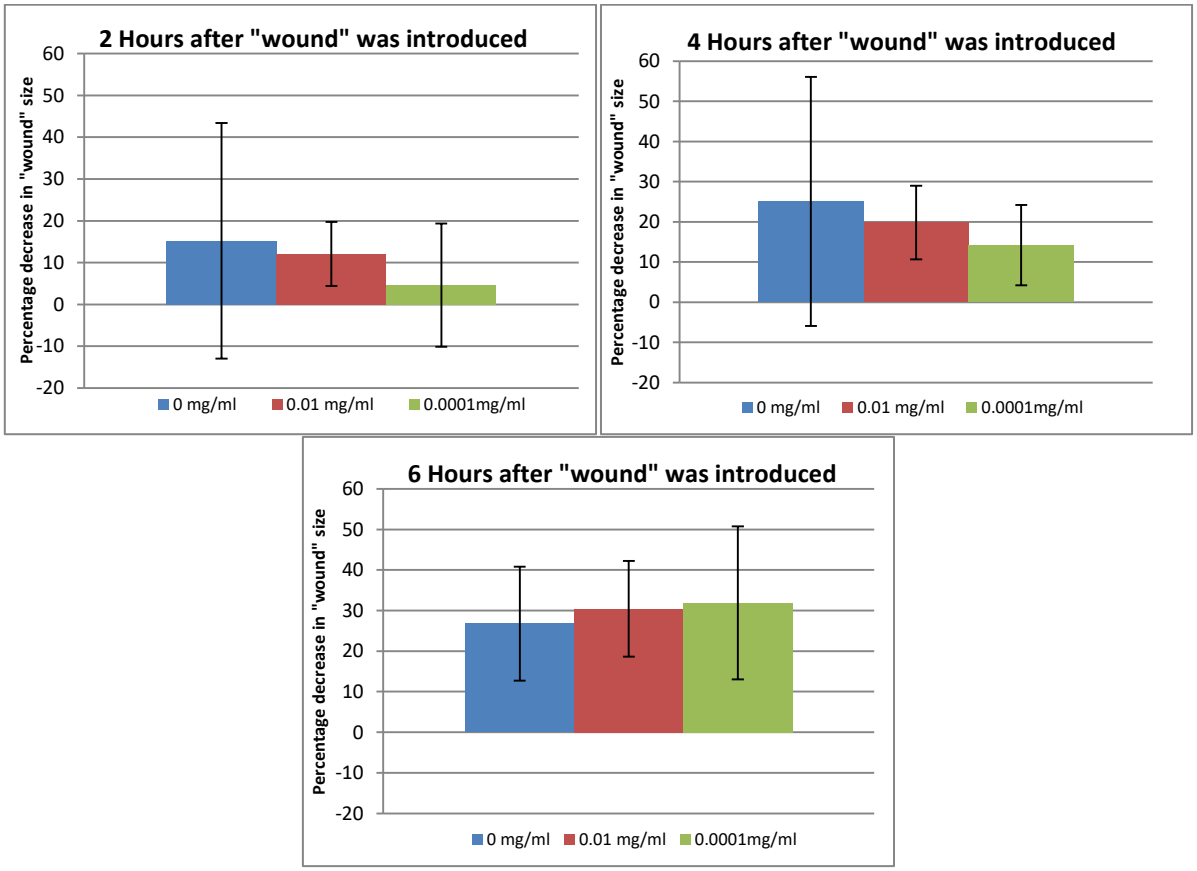

Figure 5.3.1: Cell migration of coted 2D surface. *Percentage decrease in wound size over a 24 hour period, for 0.01 mg/ml and 0.0001mg/ml coated ESM. Cells were grown in 2D well over a period of 48 hour before "wound" was introduced. Measurements of wound size were taken at 0, 2, 4, 6 and 24 hours after wound was introduced. After 24 hours the wound had disappeared. Cells showed a much faster migration time at 0mg/ml than at either ESM concentrations in the beginning. After 6 hours the cells living on 0.01 mg/ml and 0.0001 mg/ml coated ESM showed a tenden of higher rate of migration than the control sample*

5.4: RT-PCR

5.4.1: Expression of MRFs increased during differentiation upon ESM incubation.

RT-PCR was used to estimate the change in expression of the two myogenic regulatory factors MyoD and myogenin for cells exposed to 0.01mg/ml and 0.0001 mg/ml concentrations of coated ESM (figure 5.4.1A and 5.4.1B). Cells tested while in the proliferation phase showed no significant difference in expression compare to control for either MyoD or myogenin, with only small changes in expression. Cells in the differentiation phase showed that there was significant increase compare to control at all concentrations of coated ESM, with 0.0001 mg/ml having the greatest increase. The expression of MyoD was tested at two different time points, MyoD expression was first measured after 48 hours or two days, during which the cells were only given access to proliferation medium. The second time point was after 120 hours or five days, with cells having access to the proliferation medium for the three first days before medium was changed to differentiation for the remaining 48 hours. P-values were calculated using the ΔΔCt –values from calculating fold change using the reference gene elongation factor alpha 1(EF-A1). Change in expression was also calculated using the reference gene TATA (see appendix)

MyoD

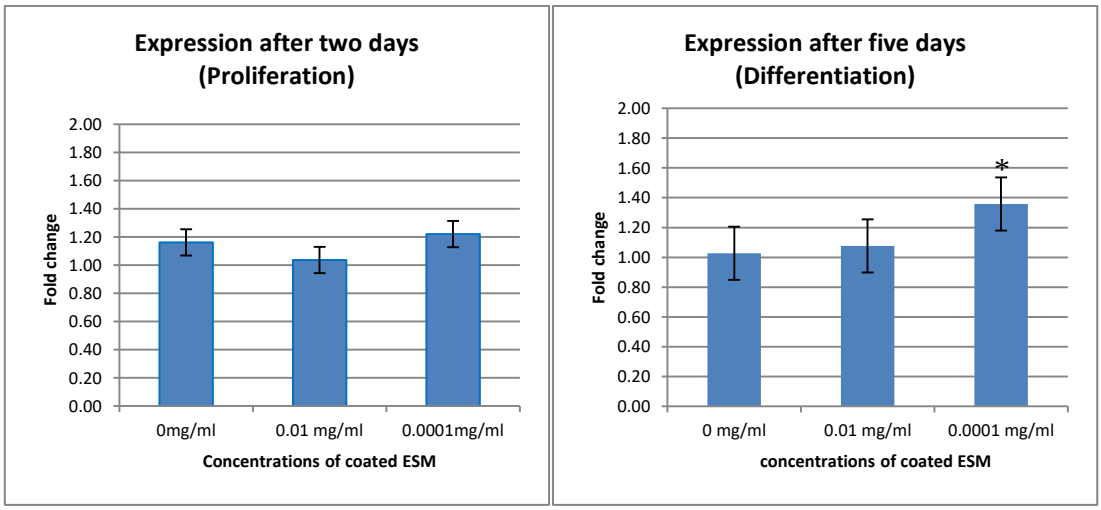

Figure 5.4.1A: Change in expression of MyoD. *Change in expression for samples introduced to coated ESM after two and five days was calculated using EF-A1 as reference gene. Cells were introduced to a 2D surface with either 0.01 mg/ml or 0.0001 mg/ml coated ESM. Change in expression was calculated using control (untreated sample) to normalize data for samples treated with coated ESM. The different values represented by the fold change denomination equals: no change (1.0), increase (>1.0) or decrease (<1.0) in expression and was calculated using the ΔΔct-values. Each individual column represents three different experiments seeded out in triplicates. There were significant differences between control and coated samples after five days(differentiation) for the expression of myoD, showing an increase in expression for cells when ESM was presents in coated form * Significant value compared to control *(p-value<0.05) and ** (p-values<0.01).*

Myogenin

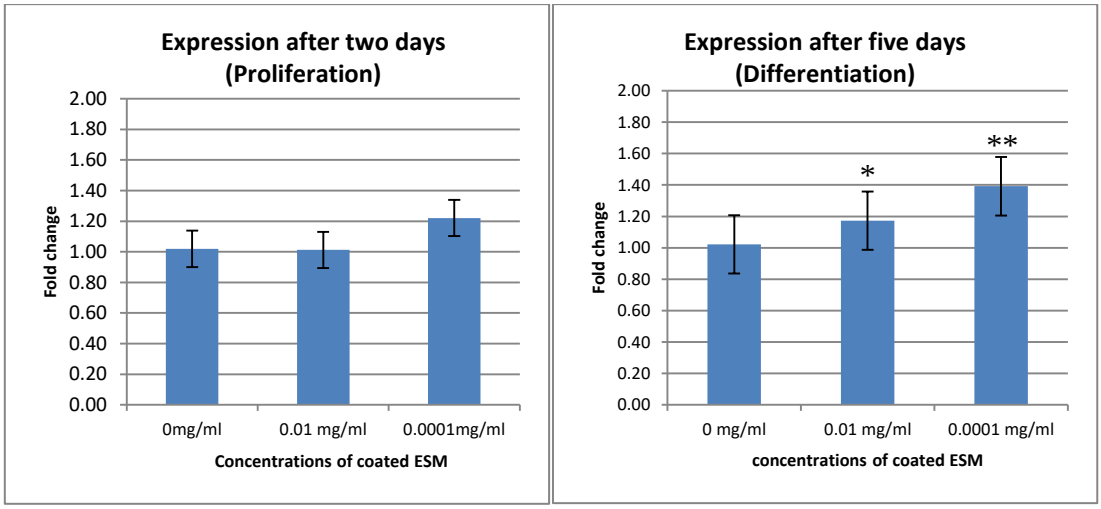

Figure 5.4.1B: Change in expression of myogenin. *Change in expression for samples introduced to coated ESM after two and five days was calculated using EF-A1 as reference gene. Cells were introduced to a 2D surface with either 0.01 mg/ml or 0.0001 mg/ml coated ESM. The different values represented by the fold change denomination equals: no change (1.0), increase (>1.0) or decrease (<1.0) in expression and was calculated using the ΔΔct-values. Each individual column represents three different experiments seeded out in triplicates. The only significant difference in myogenin expression was for cells after five days (differentiation) on coated ESM at both concentrations * Significant value compared to control (p-value<0.05). ** Significant value (p-values<0.01).*

5.4.2: The effect of ESM on the production of extra cellular matrix components

Change in expression was calculated using RT-PCR for the extra cellular matrix components: *collagen I, decorin* and *biglycan* with EF-A1 as reference gene. The experiment used similar parameters as the estimation of fold change for the myogenic regulatory factors, in which myoblast cells were allowed to interact with coated ESM over a period of two and five days. Significant changes in expression was calculated for *collagen 1* (figure 5.4.2A) during the differentiation phase of the cell at both tested concentrations. There was also a significant change in the expression for *decorin* (5.4.2B) during cell differentiation, but only for cells interacting with coated ESM at concentrations of 0.0001mg/ml. There was no significant change in expression in *biglycan*. P-values were calculated using the ΔΔCt –values which had been calculated to estimate fold change. Change in expression was also calculated using reference gen TATA (See Appendix)

Collagen

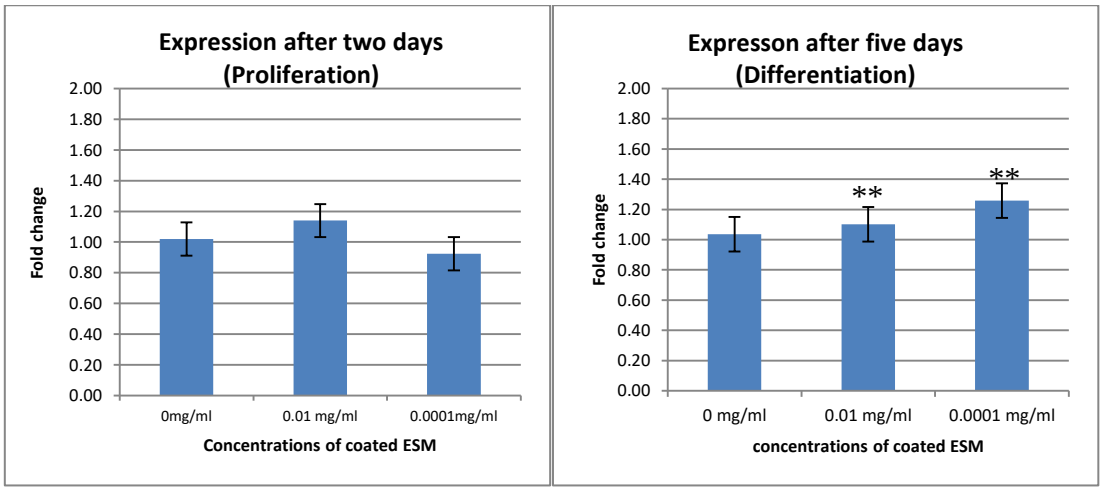

Figure 5.4.2A: Change in expression of Collagen type I. *Change in expression for samples introduced to coated ESM after two and five days was calculated using EF-A1 as reference gene. Cells were introduced to a 2D surface with either 0.01 mg/ml or 0.0001 mg/ml coated ESM. Change in expression was calculated using control (untreated sample) to normalize data for treated samples. The different values represented by the fold change denomination equals: no change (1.0), increase (>1.0) or decrease (<1.0) in expression and was calculated using the ΔΔct-values. Each individual column represents three different experiments seeded out in triplicates. The only significant change in expression was for cells in the differentiation phase for both concentrations. * Significant value compared to control (p-value<0.05). ** Significant value (p-values<0.01).*

Decorin

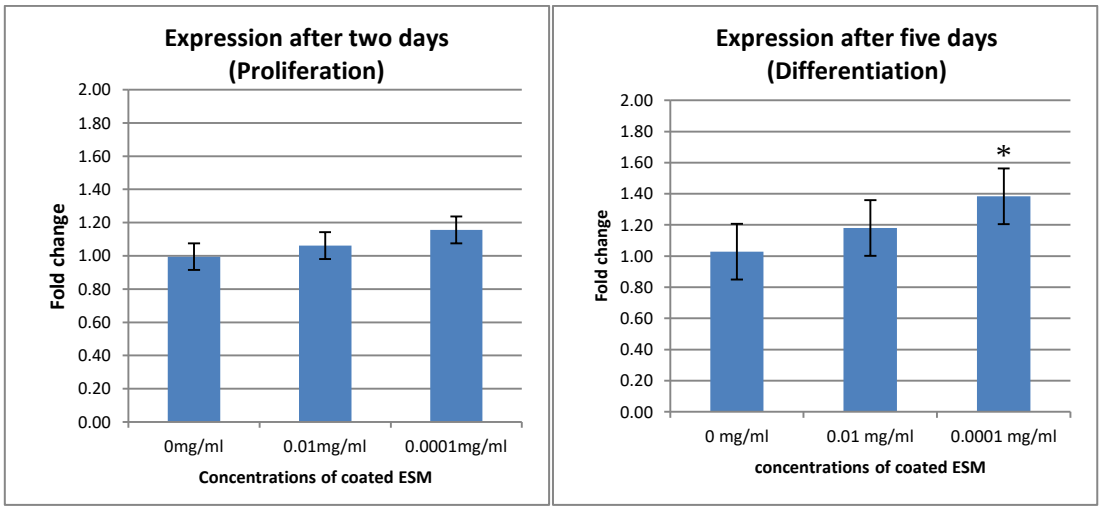

Figure 5.4.2B: Change in expression of decorin. *Change in expression for samples introduced to coated ESM after two and five days was calculated using EF-A1 as reference gene. Cells were introduced to a 2D surface with either 0.01 mg/ml or 0.0001 mg/ml coated ESM. Change in expression was calculated using control (untreated sample) to normalize data for treated samples. The different values represented by the fold change denomination equals: no change (1.0), increase (>1.0) or decrease (<1.0) in expression and was calculated using the ΔΔct-values. Each individual column represents three different experiments seeded out in triplicates. The only significant values were for cells in the differentiation phase, with 0.0001 mg/ml showing increase in expression. * Significant value compared to control (p-value<0.05). ** Significant value (p-values<0.01).*

Biglycan

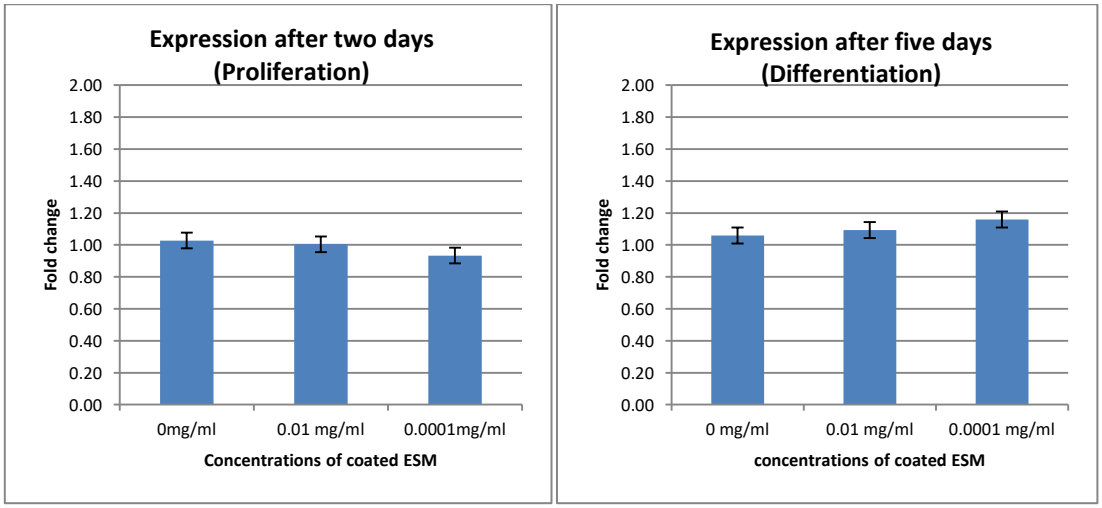

Figure 5.4.2C: Change in expression of biglycan. *Change in expression for samples introduced to coated ESM after two and five days was calculated using EF-A1 as reference gene. Cells were introduced to a 2D surface with either 0.01 mg/ml or 0.0001 mg/ml coated ESM. Change in expression was calculated using control (untreated sample) to normalize data for treated samples. The different values represented by the fold change denomination equals: no change (1.0), increase (>1.0) or decrease (<1.0) in expression and was calculated using the ΔΔct-value. Each individual column represents three different experiments seeded out in triplicates. There was no significant change in expression for any sample. * Significant value compared to control (p-value<0.05). ** Significant value (p-values<0.01).*

5.5: The expression of decorin increased when cells were exposed to ESM.

Two different 3D scaffolds (ESM and collagen) were tested to investigate if muscle cells were able to proliferate and differentiate while interacting with the scaffolding structure. The two different scaffolds used was the control scaffold containing collagen only (0.75% collagen) and ESM scaffold containing a mixture of ESM and collagen (3% ESM and 0.75% collagen). For cells tested during proliferation, there was no significant differences in expression of neither MyoD nor myogenin compared to control (α=0.05 and 0.01) and only decorin showed a modest increase in fold change. For cells tested during differentiation, only decorin expression increased significantly (p-value<0.05 and 0.01).

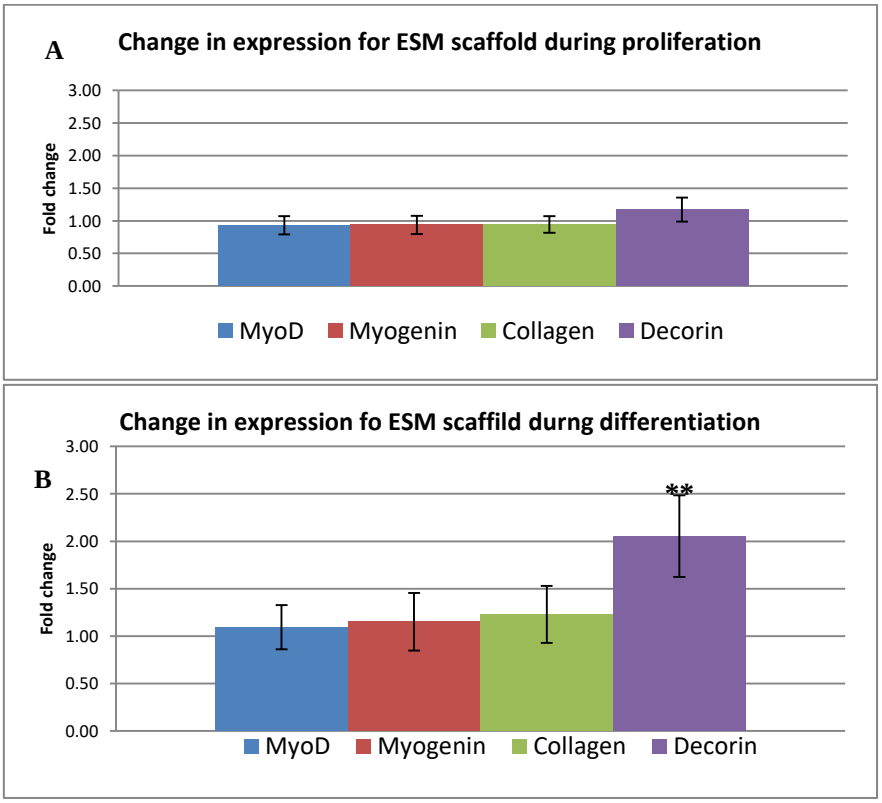

Figure 5.5: Change in expression for cells growing on 3D-scaffolds. *Fold change or change in expression estimated for cells growing on ESM scaffolds (3% ESM and 0.75%) by comparing ct-values of the ESM scaffold to the control scaffolds (0.75% collagen). A) Calculated fold change for myoblast cells living on ESM scaffold over a period of seven days with proliferation medium. B) Calculated fold change for myoblast cells living on ESM scaffold for a period of twenty days with proliferation medium for seven days, and 13 days with differentiation medium. Data presented as mean+SD. Only **Decorin after twenty days showed a significant difference in expression compare to control (*p-value<0.05 and **0.01) p-value was calculated using the ΔΔCt-values. Values were calculated using data from two replicates of each gene, which was measured twice for each experiment. A total of three experiments were conducted measuring gene expression for cells interacting with the scaffold during proliferation and differentiation.*

5.6: 3D Scaffolding and Cell migration

The ESM and collagen scaffold was sliced into layers and stained with immuno-fluorescent antibodies, making it possible to observe cell-scaffold interaction during proliferation and differentiation, as well as the structural composition of the scaffold.

5.6.1: Structure of the ESM and collagen scaffold

The structure of the ESM and collagen scaffold was observed using immuo-fluorescent WGA antibodies. It was noted that the structural composition of the scaffold containing ESM seemed more open in comparison to the structure of the collagen scaffold, small flacks of powdered ESM was also observed to be spread about inside of the structure of the ESM scaffold. When a single component of the ESM scaffold was observed more closely, a fibrous like network structures could be seen, making up the primary architecture of the ESM flack (figure 5.6.1B).

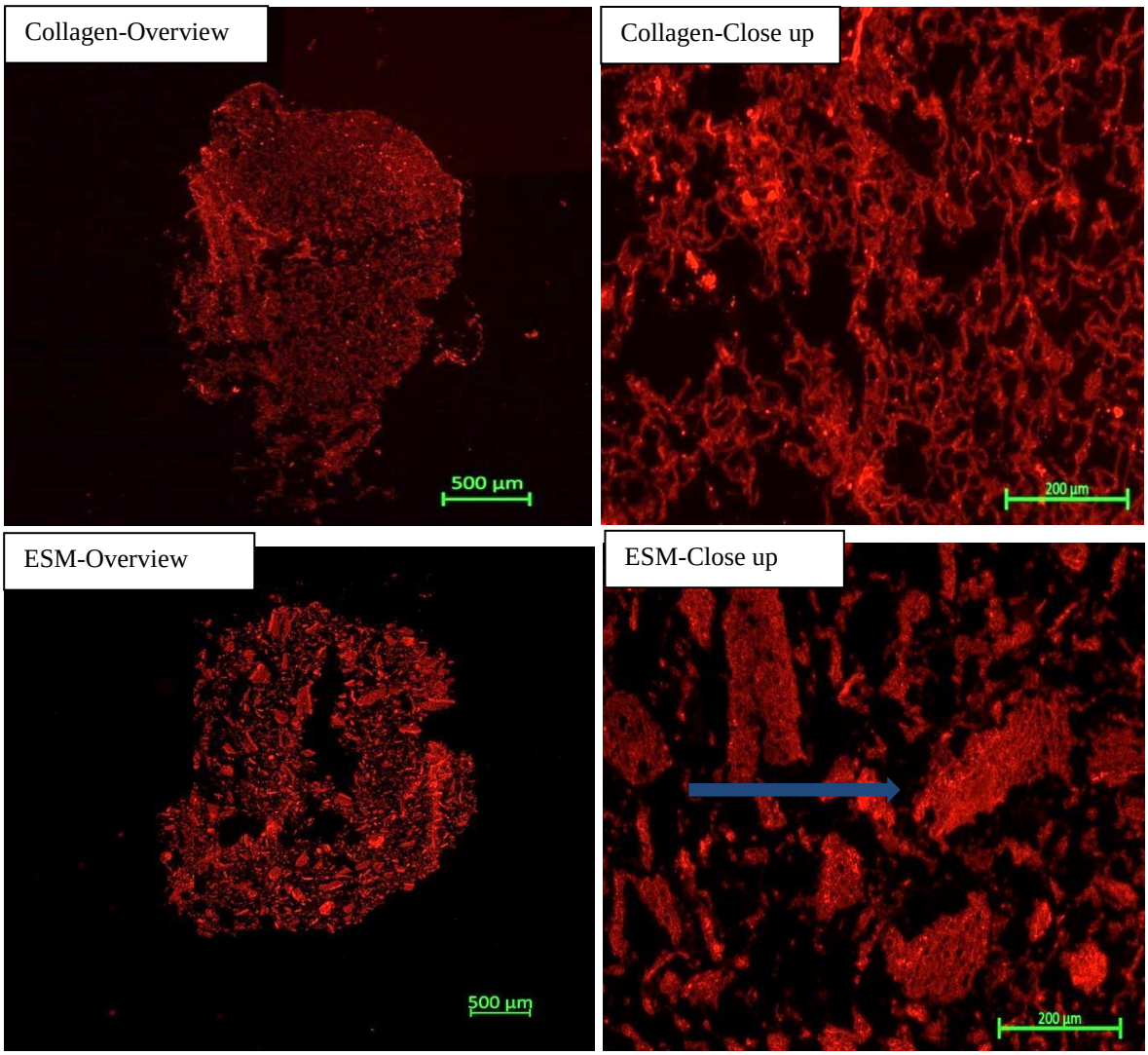

Figure 5.6.1A: Structural overview of the ESM and collagen scaffold. *The 3D structure was stained with WGA-594 (red) antibodies, which attach itself to positively charged structures in the scaffold. Images were processed using the ZEISS Axio Observer Z1 microscope. The structural overview of the ESM and collagen scaffold is shown with the differences in architectural composition between the two scaffolds. Blue arrow shows a single ESM component inside of the ESM scaffold. Images are not directly relatable to each other and only serve to show the difference in structure and architectural composition.*

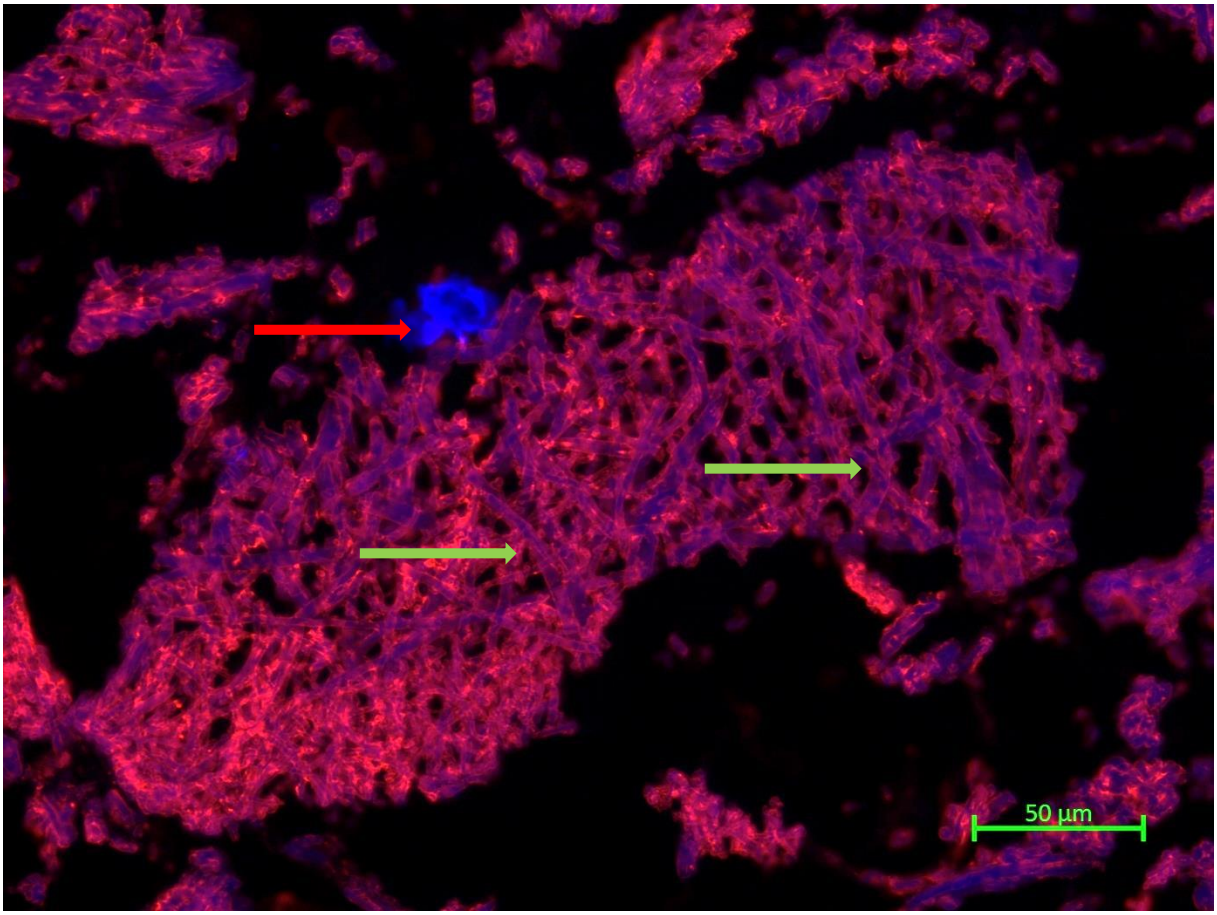

Figure 5.6.1B: Structure of the ESM in a 3D scaffold. *The architecture of a single ESM-flack in the 3D scaffold was colored using WGA-594(red) antibodies that interact with the positively charged structures of the ESM, while myoblast cells were stained with the dapi-Hoechst (blue) antibodies.Picture was taken using the Microscope Axio observer Z1 and processed using the ZEN blue picture program. Close up of a single flack in the ESM scaffold, showing the interconnected fibril network. The red arrow shows a single cell that is interacting with the ESM-flack. Green arrows show the fibrous network like structure of the ESM - component.*

5.6.2: Cell migration and structural interaction

It was observed that cells interacting with ESM scaffold were able to migrate further inside the 3D structure than cells interacting with the collagen scaffolds (figure 5.6.2A). Further it was observed that cells interacting with the collagen scaffold would accumulate around the edges, with only a few cells being able to migrate into the 3D structure. A closer look of the ESM scaffolds (figure 5.6.2B) showed that cells were able to interact with the ESM components and that the muscle specific protein, NCAM, was present on the cell membrane.

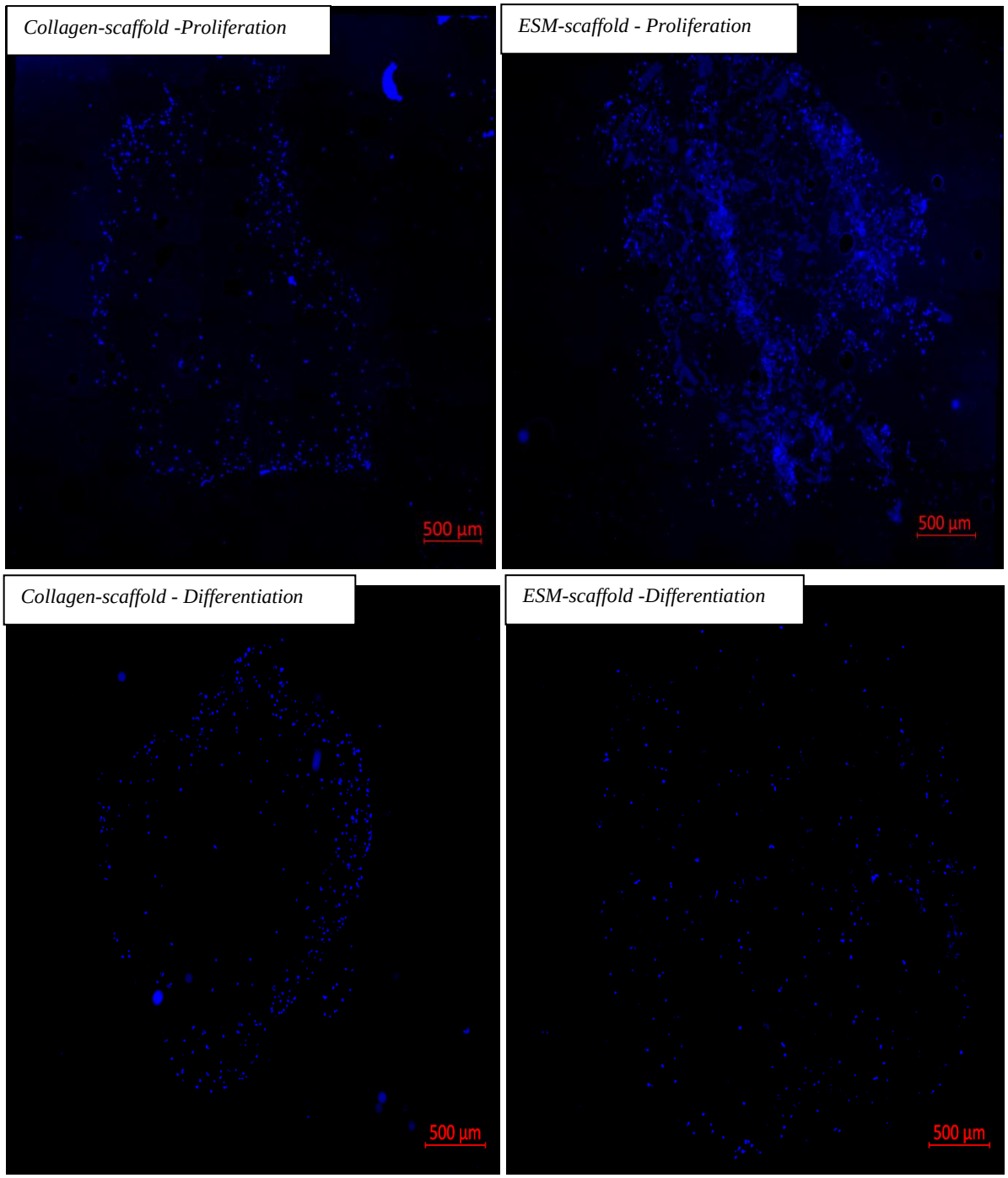

Figure 5.6.2A: Collagen and Eggshell membrane scaffold. *Images show ESM and collagen scaffold slices. Scaffolds were coloured using the dapi blue, Hoechst. Pictures was taken using the Microscope Axio observer Z1 and processed using the ZEN blue picture program. Further processing of images was done through the programme imageJ. Cells can be observed as blue dots in the pictures, large concentrations of cells can be observed as a blue patch. Cells were observed to be more willing to migrate inside the 3D structure of the ESM scaffold, than to migrate inside the 3D structure of the collagen scaffold. Pictures were taken for cells while in the proliferation and differentiation phase.*

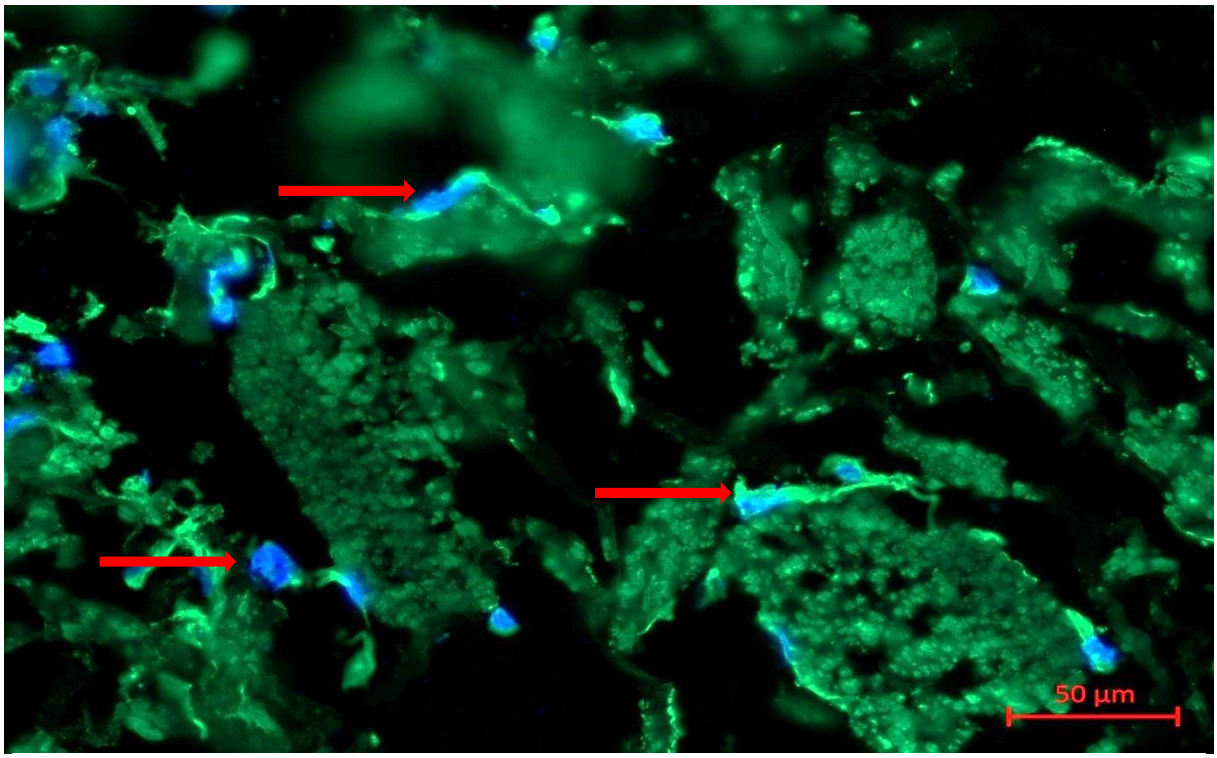

Figure 5.6.2C: Interaction between the ESM scaffold and myoblast cells. *The ESM scaffold was stained with dapi-hocehst (blue) and the mouse (anti-NCAM) with conjugated alexa-488 (green).Picture was taken using the Microscope Axio observer Z1 and processed using the ZEN blue picture program. Further processing of images was done using the programme imageJ. Red arrows shows cell interacting with the ESM scaffold. Cells had been fixated using liquid nitrogen while in the proliferation phase.*

6: Discussion

A possible solution to the lack of available tissue and organs for transplantation is to engineer the desired tissue, this could provide a long-term solution to the increasing lack of donors, and reducing the risks associated with receiving a transplant from another person. The primary method when engineering tissue is to use a 3D-scaffolding structure to support and direct cell growth, using the recipients own cells to form the tissue.

The primary approach in 3D tissue engineering is to use a biomaterial that can mimic the role of the ECM during tissue formation. Many different biomaterials has been proposed to be used in tissue engineering, there are however drawbacks with many of these materials, such as cost, availability, quality and performance (O'brien, 2011). It is preferable that a biomaterial share several similarities with the ECM, as it has to be able to fulfil several of the same roles. A material that is showing great potential is the eggshell membrane (ESM) due to its similarity in both composition and structure to the ECM (Baláž, 2014).

The aim of this study was to observe the effects of ESM on muscle cells isolated from the sirloin of a newly slaughtered bovine in 2D and 3D environments.

6.1: The Effect of ESM on viability, proliferation and cytotoxicity.

The effects of the ESM material on myoblast proliferation, viability and cytotoxicity were tested with concentrations ranging between 0.0001-5 mg/ml. The ESM material was presented to cells in the forms of free, coated, hydrolyzed and mixed ESM.

6.1.1: Cell performance was reduced by the addition of free ESM

Free ESM was presented to myoblast cells at concentrations ranging from 3 to 0.1 mg/ml. Proliferation and viability was decreased for all tested concentrations, coupled with an increase in cytotoxicity.

Previous studies conducted at Nofima had shown that proliferation rates of fibroblast cells was improved with the addition of ESM, when administrated freely onto the samples at concentrations of 1 and 3 mg/ml, with only minor toxic effects (Wilhelmsen, 2017). This was however not the case when working with myoblast cells, which was negatively impacted by the addition of free ESM. The effect of free ESM on myoblast performance is not known, but the approach used to introduce the material could have impacted cell performance. It is possible that myoblast cells are sensitive to the approach used to present the ESM material, or

that the approached used was too disorganized for cells to properly interact with the material. During normal tissue formation the ECM, which the ESM material is supposed to mimic, goes through several rounds of modifications, and structural changes, these changes can impact cell behavior and induce biological processes, which shows that cells are sensitive to structural differences (Theocharis et al., 2016). Structural defect in the ECM during tissue formation can also lead to scaring or to degradation of tissue, myoblast cells in are sensitive to changes in the structure of the ECM, as they depend on the matrix for different biological processes and the correct formation of myofibers (Goetsch et al., 2003). It seems that the addition of free ESM had an overall negative impact on the performance of myoblast cells in the 2D environment.

6.1.2: Hydrolyzed and mixed ESM negatively impacted cell performance.

Samples containing hydrolyzed ESM had the clearest decrease in proliferation and viability, coupled with an increase in cytotoxicity. Higher concentrations of hydrolyzed ESM seemed to correlate with an overall decrease in myoblast performance.

It was concluded based on these measurements that the addition of hydrolyzed ESM negatively affected myoblast performance, and further testing was not conducted. The negative impact of hydrolyzed ESM could be a result of the processing method used on the material, which introduced major changes, that could have made it undesirable for the cells to interact with (Ohto-Fujita et al., 2011). It is also possible that structural changes to the ESM allowed the material to obtained new properties, which negatively impacted cell performance (Ohto-Fujita et al., 2011).

It has been observed that hydrolyzed material has the ability to partially self-reassemble into new structures (Ohto-Fujita et al., 2011). Reassembly of hydrolyzed units is common when the hydrolyzed material is present in high concentrations, increasing the possibility that some parts will interact to form new structures. The reassembly of some ESM structures could create an uneven distribution between partially reassembled, and hydrolyzed ESM that may have had a negatively impact on cell performance (Ohto-Fujita et al., 2011). The assembly of new structures in the sample could affected how the material interacted with myoblast cells, creating new functions and abilities for the material, which negatively impacted cell performance (Ohto-Fujita et al., 2011).

Unrelated studies on the hydrolyzed ESM material conducted at the university of Osaka, using different concentrations of alkaline-digested ESM ranging between 0-100 mg/ml on fibroblast cells, showed that the cell were able to interact with the hydrolyzed ESM material, creating an functional 2D environment that mimicking the ECM *in vitro* (Ohto-Fujita et al., 2011). However, the ESM material was conjugated to the surface of the culture vessel using Poly (MPC-co-BMA-co-MEONP) when presented to the cells, and not blended with the cell medium as in this study (Ohto-Fujita et al., 2011). It was also shown that the hydrolyzed ESM material would adopt a fibrillary structure when conjugated to the surface, this structure is described as being dose dependent on the ESM (Ohto-Fujita et al., 2011). Further was it shown that cells would adopt different adhesion modes after the amount of ESM present in a sample (Ohto-Fujita et al., 2011). Studies conducted at Nofima using hydrolyzed ESM had also shown that fibroblast performance was improved by the addition of hydrolyzed ESM, with an increase in proliferation (Kristiane, 2017). This seems to indicate that fibroblast cells are better suited to interact with the hydrolyze ESM material compare to myoblast cells and that the effect of the ESM material on cells seems to be both dose and morphologically dependent.

6.1.3: Cells prefer coated ESM.

Myoblast cells interacting on coated ESM showed an overall decrease in proliferation and viability, with an increase in cytotoxicity for concentrations ranging between 0.1 -3 mg/ml. For concentrations at 0.01, 0.001 and 0.0001 mg/ml there was no significant impact on proliferation and viability, but there was a decrease in cytotoxicity. These results showed that coated ESM was less cytotoxic to myoblast cells when presented 0.01, 0.001 and 0.0001 mg/ml concentrations.

The positive effect of coated ESM on cell performance is uncertain. However, it can be speculated that the approach used to present the ESM material was beneficial for the cells in that it may have provided a more similar environment to that found in the ECM, thus ensuring better conditions for the cell (O'brien, 2011). The reduction in myoblast performance at higher coated ESM concentrations could be due the culture vessel surface contained too much ESM, creating an uneven topography that made it difficult for the cells to interact with the material.

A difference between coated ESM and other approaches was that coated ESM was present on the surface of a culture vessel before the addition of cells, while other approaches would introduce the ESM material after cells have had some time to adhere to the surface. This variance in how cells interacted with the material could have affected cell performance, but precise effect is uncertain.

Due to the improved effect of coated ESM on myoblast cytotoxicity, without reducing proliferation or viability at 0.01, 0.001 and 0.0001 mg/ml further experiments during this study in 2D environments was conducted using coated ESM.

6.1.4: Cell performance seems to be dictated by topological features.

As previously mentioned the formation of tissue *in vivo* has been shown to be highly depended on the topographical features of the ECM (Theocharis et al., 2016), with the components of the ECM inducing and regulating cell interaction (Ostrovidov et al., 2014). It could be argued that coated ESM presents a more orderly structure for which the cells can interact with, and that the method used is more similar with how cells would interact with the ECM during *in vivo* conditions (Badylak, Freytes, & Gilbert, 2009). This could also explain why cells seems to perform poorly when interacting with more disorganized methods of presenting the ESM material, which could reduce cell performance due to cell being unable to interact with the material in an preferable way (Badylak et al., 2009; Frantz et al., 2010). The reduced performance at higher concentrations of coated ESM could be in relation to the surface of the culture vessel being too saturated with ESM, creating an uneven surface topography, which may have made it difficult for cells to correctly interact with the material.

6.2: Cell migration in a 2D environment is improved by the addition of ESM.

It was observed that cell migration was affected by the addition of coated ESM material in a 2D environment. The impact of the ESM material seems to be reflected in a faster migration rate over a prolonged period of time. Migration rate for cells interacting with the coated ESM material seems to be slower at the beginning of the experiment, but overtakes the control at later time periods. Cell migration was observed after 2 and 4 hours, which showed that cells interacting with the ESM were slower to migrate into the wound, however, after 6 hours cells living on coated ESM at had overtaken the control group.

The primary reason for this difference in migration rate between control and coated ESM samples remain unknown, however, it has been established that collagen, which is an component of the ESM (Wilhelmsen, 2017), can initiate migration for human dermal fibroblasts together with different growth factors (Li et al., 2004). Components such as proteoglycans (PG) has also been shown to affect cells migration, using their GAG side chains, when presented as a component of the ECM, it is possible that PGs in the ESM has a similar function when interacting with myoblast cells (Sah & Rath, 2016; Theocharis et al., 2016). Cell behavior during 2D studies differ from the normal behavior of cells in 3D environments, however, 2D experiments are still an important source of information about how different molecules can impact cell migration, matrix remodeling and other cellular processes (Yarrow et al., 2004).

6.3: Cell migration in a 3D environment.

The 3D scaffold experiments showed, using immuno-fluorescent staining, that cells were able to migrate into the ESM scaffold. Two primary differences were observed between the ESM and collagen scaffold; first, more cells would migrate further into the ESM scaffold, and second, cells would be more evenly distributed in the ESM scaffold. For the collagen scaffold it was observed that cells accumulated in bundles on the surface of the structure, and that cells would stay close to the surface with only a migrate into the interior.

The difference in myoblast behavior when interacting with the ESM scaffold in comparison to the collagen could be due to structural and compositional differences between the two materials. The architecture of the ESM scaffold could be observed through a microscope using fluorescent WGA-antibodies, which showed that the structure was composed of small ESM fragments spread unevenly throughout the 3D structure. Close up of a single ESM fragment showed that the fibril structure of the ESM was retained, and also that cells were able to interact with the material. Further it was observed that more cells would migrate into the interior ESM-scaffold. It can be speculated that the architecture of the ESM scaffold made it easier for the cells to interact with the material, which in return made the interior of the structure more accessible. Another possibility was that the presences of ESM fragments encourage cells to migrate into the scaffold, this may be due to the material containing different components, that could have promoted cell migration and different cellular processes in the ECM (Sah & Rath, 2016).

The composition of the ESM has been shown to contain several components such as collagen type I, PG and HA, which are known to promote and regulate cell behavior (Theocharis et al., 2016). It has already been shown that the architectural composition of the ECM is essential for proper cell function, tissue formation and cell-ECM interaction (Badylak, 2007). It could be that the composition of the ESM makes it possible for cells to interact with the material in a similar fashion as to when cells interact with the ECM. The ESM shares many similarities with the ECM in that both have fibrous network consisting mostly of collagen, with PG and HA components, reflecting the similar role the two materials have in their respective environment; structural support, cellular process and protection (Baláž, 2014). While collagen is an essential part of the structural composition of the ECM, and have been shown to play an essential part in tissue formation and regeneration, the lack of compositional diversity in the collagen scaffold, missing components such as GAG, PG and HA which have been shown to be essential during myogenesis and regeneration, could have reduced cells ability to interact with the collagen scaffold (Sah & Rath, 2016).

Several different properties for the ESM- scaffold was observed during this study which could help shed some light on some of the possible applications of the material. It was observed that the collagen scaffold would degraded at a much higher rate than the ESM scaffold, this was particularly prominent when studying myoblast-scaffold interaction during the differentiation phase, as scaffolds were kept in test conditions for twice as long, compare to cells tested during proliferation. Several collagen scaffolds would degrade to a point where it was no longer possible to slice them into smaller pieces for immuno-staining. It was also observed that the collagen scaffold proved rather fragile when handled, as it would easily bend or break when force was applied, making it difficult to work with. In comparison the ESM scaffold proved fare more robust when handled as it was fare more able to withstanding physical pressure. The ability to withstand pressure and rate of degradation was not measured during this study and all mentioned differences were only observed while working directly with the material. While these observations shed some light on some of the differences of the ESM scaffolds in comparison to the collagen scaffold, with the ESM scaffold seeming to be more able to withstand pressure and slower to degrade, these factors could make the ESM material well suited for *in vitro* tissue engineering.

6.4 Myogenic regulatory factors.

There was a significant up-regulation in the expression of the two MRFs: MyoD and myogenin, for cells interacting with powdered ESM, when it was presented as a component of the cell-adhesion matrix in a 2D environment. These two genes belong to the MRFs-group of regulatory proteins, and are essential for different parts of the myogenesis.

Cells entering into differentiation have been shown to express MyoD, giving rise to the hypothesis that it serves as a molecular switch, turning on differentiation (Sabourin & Rudnicki, 2000). Myoblasts-mutants unable to express MyoD would go through several rounds of proliferation before expiring, without the formation of any muscles (Sabourin & Rudnicki, 2000). Myogenin on the other hand is central for the formation of myotubes, as myogenic committed cells lacking the myogenin-gene has been shown to be unable to form normal muscle fibers (Sabourin & Rudnicki, 2000).

Considering that MyoD is known to be expressed during the early parts of differentiation, any increase in expression could be related to the initiation of differentiation(Bentzinger et al., 2012). It could be speculated that an up-regulation of MyoD and myogenin, display a difference in how cell interact with the ESM, with a possible effect being that cells initiate differentiation at an earlier stage, allowing for the earlier formation of myotubes, which could be reflected in the increased expression of MyoD and myogenin in comparisons to control. It was observed in related experiments conducted during this study that myoblast cells interacting with the coated ESM material would start to differentiate earlier stage, than cells lacking access to the material. It has been shown that different materials can affect or initiate differentiation, studies that showed that the addition of complex surface coating containing several ECM components significantly affected the early differentiation phase of cells in comparison to the control, or to cells that only interacted with a single ECM component (Rønning et al., 2013).

Since the composition of components seems to affect cell behavior, with compositions closer to the ECM seems to impact differentiation more, it could be speculated that the complex structural composition of ESM, which is both similar to the ECM in composition and architecture could impact cell differentiation. There is also a relationship between the different developmental stages of tissue and ECM formation, as it has been shown that the ECM goes through several modifications through its existence, with changes in composition and architecture cell behavior differently, and that the composition of the ECM influence

tissue development, however the precise method of how this function is yet unknown (Ohto-Fujita et al., 2011). The amount of estimated MyoD and myogenin mRNA may have been affected by samples induced to differentiation still containing proliferating cells, producing a more significant change in expression for MyoD and myogenin. The increase in expression of decorin, which is a structural protein found in the ECM, could be related to the formation of myotube, as myoblast cells forms into myotubes it has been shown that there is an increase in expression of structural proteins (Rønning et al., 2013).

6.5: Extra cellular matrix components.

The expression of the ECM components; collagen type I, decorin and biglycan, was measured using RT-PCR, for cells in 2D and 3D environments. It was observed that myoblast cells interacting with coated ESM in 2D environment had a significant increase in the expression of collagen type I and decorin during differentiation. The expression of decorin was also significantly increased for cells interacting with the ESM scaffold during differentiation. There was no significant increase in expression for any ECM component during proliferation for myoblast cells in either 2D or 3D environments.

The increase in expression of collagen type I and decorin for myoblast cells in 2D environments could be as a result of the formation of a new native ECM. Both collagen and decorin has been shown to be central components of the ECM, as collagen is the primary network forming protein found in ECM (Theocharis et al., 2016), while decorin is known to assist on how the fibrous network is arranged and organized (Casar et al., 2004). The increased expression of decorin for cells interacting with the ESM scaffold could be similar to the previous statement, with cells trying to organize and form new native ESM. The difference in expression of collagen in 3D compare to cells in 2D environment, could be due to how the ESM is presented in the scaffold, with the scaffold being more in-line with how the native ECM would have been presented to the cells. Overall the increase in expression is most prominent during differentiation, which could indicate that the formation of new ECM is most common during this cell phase, it has been shown that the ECM goes through several rounds of modifications during tissue formation (Frantz et al., 2010), and that the increase in expression of different components is simply and attempt of the cells to modify its surrounding environment.

6.6: Methodical issues

The results of this study have assisted in providing further insight into the interaction between myoblast cells and the eggshell membrane in both 2D and 3D environments The different methodical issues that were encountered during this study will be presented systematically from the first to last conducted experiment during this part of the paper.

During myoblast isolation, fibroblast cells would manage to remain in isolated myoblast cell cultures after attempts of removal; previous studies had shown that around 10% of isolated cell culture would be fibroblast cells (Rønning et al., 2013). The fibroblasts proved more able than the myoblast cell, and could overtake the cultures if the culture was split too many times or kept over a long period of time; this would change the fibroblast:myoblast ratio in the sample and thus render the samples useless. The impact of the presence of fibroblast cells during the study was not measured, however due to the method used to isolate myoblast cells in large quantities, small samples of fibroblast cells would always be present in the myoblast samples. It should be noted that *in vivo* tissue would have fibroblast present at all times in muscle structures, making fibroblast cells a natural part of the muscle environment.

Cell cultures on the 2D surface did not behave as the cells would have done in normal *in vivo* conditions, as myoblast cells would form serval anchoring points on the surface when adhering, which would lead to the formation of branched myotubes, a structure that is not normally observed in normal *in vivo* conditions. It is not known how this affected cells performance during this study (Rønning et al., 2013).

Not all approaches for ESM was tested with similar concentrations, as coated ESM was tested with concentrations ranging between 3-0.0001 mg/ml, while hydrolyzed ESM was tested with concentrations ranging between 5-0.01 mg/ml.

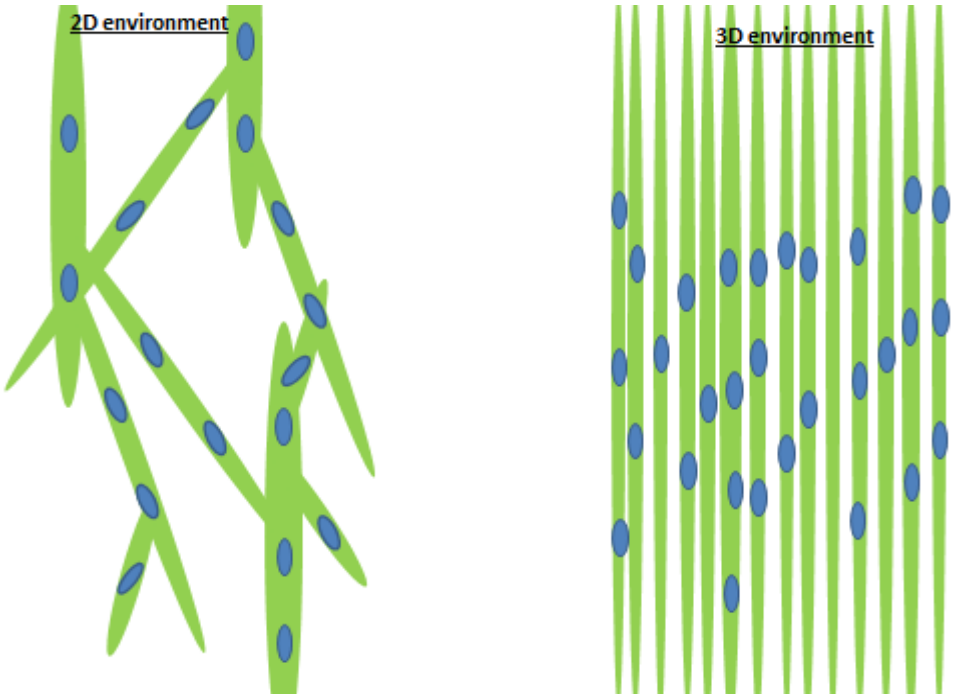

Figure 6.5A: muscle cells in 2D and 3D environments. *Muscle cells in 2D environments would form branched, structures, something that is not observed in 3D environments. Green represents the overall structure of the cell, while blue represents the cell nucleus.*

Working with the ESM material in ESM form showed that ESM, when administrated freely into a 2D culture vessel, would accumulate in the center of the culture vessel after a certain period. This accumulation would create an uneven distribution of the material, with high concentrations of ESM in the center, and lower concentrations at the edges. As a consequence of the uneven distribution of ESM, observing cells during proliferation proved difficult as the material would block the view in areas with high accumulation. It was also observed that cells would migrate towards areas containing ESM, which would help to obscure the cells, particularly at high concentrations. There were also some difficulties with isolating mRNA from samples containing free EMS, due to material clogging the RNA filters during the purification process. There were attempts to separate the ESM from the sample before filtration however at high ESM concentration small quantities of the material would still remain during filtration. The impact of ESM on the amount of mRNA isolated was not estimated, and free ESM was not worked with further.

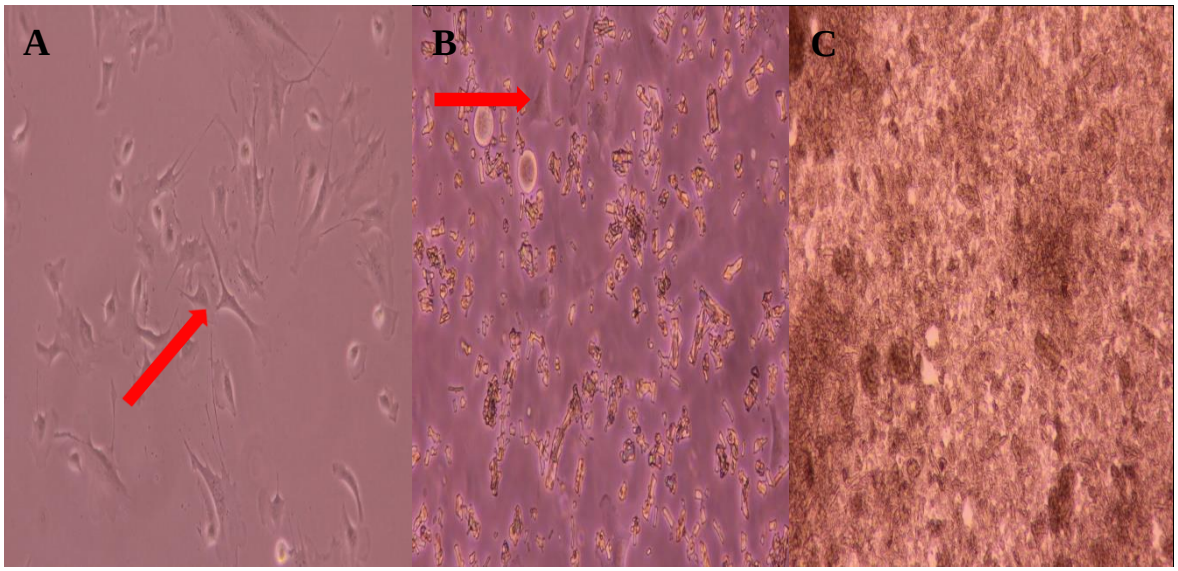

Figure 6.5B: The distribution of free ESM in culture vessels. *The difference in distribution between 0mg/ml (A), 1 mg/ml (B) and 3 mg/ml (C) ESM material in the culture vessel. Red arrows show the presents of cells, which were only observable at concentrations 1 mg/ml or lower. All images were taken during this study using the Microscope Leica DMIL LED.*

Only coated ESM was used in further 2D experiments due to the poor performance of myoblast cells interacting with free, hydrol and mixed ESM. This ensured that cells were not tested on these ways of presenting the ESM material during differentiation. Studies have shown that the addition of ECM components to cells can have the greatest impact during differentiation, and this seemed to correlate with observations made during this study (Ostrovidov et al., 2014). Testing myoblast cells on free ESM, hydrol and mixed during differentiation would have been preferable to observe any effects during this phase.

The creation of the wounds during the cells migration experiment was done in an uneven manner, as to much force was administrated at certain locations, creating uneven distances across the wound. There was also a great variety in how cells would migrate into the wound-area with certain cells preferring to migrate across in a bridge-like formation. The difference in wound size and the uneven migration pattern are the primary reasons for the high standard deviation shown (figure 5.3.1) during the study.

Calculating the change in expression of cell using RT-PCR has been proven to be an effective method for accurate measurements for the change in expression (Kralik & Ricchi, 2017). Data provided by RT-PCR was normalized towards the reference gen, and significant outliers were removed. Since RT-PCR is an incredible sensitive procedure, even small differences in samples preparations can create vast differences in-between data, to reduce the amount of

error, several experiments were conducted to ensure that there was an abundance of data available to reduce the error rate and deviation.

The 3D scaffolds did not have any systems in place for the transportation of nutrients into interior of the structure, which could have affected the survivability of cells that had migrated into the scaffold. Scaffold size was reduced to ensure that medium was able to seep into the structure, giving cells access to nourishment. There was a significant difference in size between the collagen and ESM scaffold due to degradation of the 3D structure when exposed to testing conditions over prolonged periods of time. The rate of degradation was much higher for the collagen scaffold, and when the scaffolds effect on differentiation was tested, it was observed that the overall structure of several collagen scaffolds had degraded so much that it was impossible to use them in immuno-fluorescent staining.

7: Conclusion

This study tested the effects of ESM on myoblast cells during the proliferation and differentiation, with a focus on how the addition of ESM material to 2D and 3D environments improved tissue generation for skeletal muscle structure by mimicking the role of the ECM. The 2D effects of ESM on proliferation, viability and cytotoxicity were tested. RT-PCR was conducted for cells in both 2D and a 3D environment with immune-staining using fluorescent antibodies to observe cellular activity.

It was concluded form the 2D study that the optimal way of presenting ESM was as a component of the cell-adhesion matrix. It seems that myoblast cells perform better in a more structured environment, which fits well with previously published papers on the ECM, showing that cell behavior is partially regulated by the architecture of the ECM. It was also shown that gene expression was most affected during differentiation, however the reason for this remain unknown as there have been few studies that investigates cell-ESM interaction (Ohto-Fujita et al., 2011). It could however, be speculated that the addition of ESM impacts differentiation at a much greater extent than proliferation (Ohto-Fujita et al., 2011).

The 3D study showed that cells were able to migrate and interact with the ESM scaffold, with more cells observed inside of the ESM than in the collagen scaffold. The overall structure of the ESM scaffold seemed to be more available to the cells, as they were able to migrate further into the ESM scaffold, with greater distribution. Concluding that cells were able to and willing to migrate and interact with the ESM material, when presented in a 3D structure.

The study of ESM as a biomaterial in 3D tissue engineering is still far from over, more focus could be given in the future to producing ESM with different compositions of structural elements to observe its effect on tissue formation.

7.1: Further research

Studies looking further into how the tested ESM materials would perform during myoblast differentiation could be of interest. The impact of free, hydrol and mixed ESM was only tested during cell proliferation, while the majority of observed changes to cell behavior were during differentiation. More focus should also be given in the future on how the ESM material effect differentiation in 2D and 3D environments over longer periods of time.

As it is desirable to use the ESM material to mimic the role of the ECM during tissue formation, it could be of interest to attempt to change or modify the composition of the ESM material with different components native to the ECM, but not found in the ESM, to observe how cells would perform.

Literature:

Abouna, G. M. (2008). *Organ shortage crisis: problems and possible solutions.* Paper presented at the Transplantation proceedings.

Ahmed, T. A., Suso, H.-P., & Hincke, M. T. (2017). In-depth comparative analysis of the chicken eggshell membrane proteome. *Journal of proteomics, 155*, 49-62.

Alberts, B. (2017). *Molecular biology of the cell*: Garland science.

Badylak, S. F. (2007). The extracellular matrix as a biologic scaffold material. *Biomaterials, 28*(25), 3587-3593.

Badylak, S. F., Freytes, D. O., & Gilbert, T. W. (2009). Extracellular matrix as a biological scaffold material: structure and function. *Acta biomaterialia, 5*(1), 1-13.

Baláž, M. (2014). Eggshell membrane biomaterial as a platform for applications in materials science. *Acta biomaterialia, 10*(9), 3827-3843.

Bentzinger, C. F., Wang, Y. X., & Rudnicki, M. A. (2012). Building muscle: molecular regulation of myogenesis. *Cold Spring Harbor perspectives in biology, 4*(2), a008342.

Berkes, C. A., & Tapscott, S. J. (2005). *MyoD and the transcriptional control of myogenesis.* Paper presented at the Seminars in cell & developmental biology.

Bonnans, C., Chou, J., & Werb, Z. (2014). Remodelling the extracellular matrix in development and disease. *Nature reviews Molecular cell biology, 15*(12), 786.

Böttcher-Haberzeth, S., Biedermann, T., & Reichmann, E. (2010). Tissue engineering of skin. *Burns, 36*(4), 450-460.

Casar, J. C., McKechnie, B. A., Fallon, J. R., Young, M. F., & Brandan, E. (2004). Transient up-regulation of biglycan during skeletal muscle regeneration: delayed fiber growth along with decorin increase in biglycan-deficient mice. *Developmental biology, 268*(2), 358-371.

CellTiter-Glo Luminescent Cell Viability Assay. (Last Revi. 2015).

Charge, S. B., & Rudnicki, M. A. (2004). Cellular and molecular regulation of muscle regeneration. *Physiological reviews, 84*(1), 209-238.

Chen, G., Ushida, T., & Tateishi, T. (2002). Scaffold design for tissue engineering. *Macromolecular Bioscience, 2*(2), 67-77.

Coons, A. H. (1961). The beginnings of immunofluorescence. *The Journal of Immunology, 87*(5), 499-503.

Cossu, G., & Biressi, S. (2005). *Satellite cells, myoblasts and other occasional myogenic progenitors: possible origin, phenotypic features and role in muscle regeneration.* Paper presented at the Seminars in cell & developmental biology.

Frantz, C., Stewart, K. M., & Weaver, V. M. (2010). The extracellular matrix at a glance. *J Cell Sci, 123*(24), 4195-4200.

Goetsch, S. C., Hawke, T. J., Gallardo, T. D., Richardson, J. A., & Garry, D. J. (2003). Transcriptional profiling and regulation of the extracellular matrix during muscle regeneration. *Physiological genomics, 14*(3), 261-271.

Gordon, M. K., & Hahn, R. A. (2010). Collagens. *Cell and tissue research, 339*(1), 247.

Hernández-Hernández, J. M., García-González, E. G., Brun, C. E., & Rudnicki, M. A. (2017). *The myogenic regulatory factors, determinants of muscle development, cell identity and regeneration.* Paper presented at the Seminars in cell & developmental biology.

Howard, D., Buttery, L. D., Shakesheff, K. M., & Roberts, S. J. (2008). Tissue engineering: strategies, stem cells and scaffolds. *Journal of Anatomy, 213*(1), 66-72. doi:10.1111/j.1469-7580.2008.00878.x

Introduction to TaqMan® and SYBR® Green Chemistries for Real-Time PCR. (last Rev 06/2010). (pp. 17): Applied Biosystems.

Kralik, P., & Ricchi, M. (2017). A basic guide to real time PCR in microbial diagnostics: definitions, parameters, and everything. *Frontiers in microbiology, 8*, 108.

Kristiane, B. (2017). Effekten av eggeskallmembranpulver og dens derivateer på fibroblastaktivitet som er viktig for sårheling. *Online search portal "Brage" at NMBU*.

Le Grand, F., & Rudnicki, M. A. (2007). Skeletal muscle satellite cells and adult myogenesis. *Current opinion in cell biology, 19*(6), 628-633.

Lee, S.-M., Grass, G., Kim, G.-M., Dresbach, C., Zhang, L., Gösele, U., & Knez, M. (2009). Low-temperature ZnO atomic layer deposition on biotemplates: flexible photocatalytic ZnO structures from eggshell membranes. *Physical Chemistry Chemical Physics, 11*(19), 3608-3614.

Li, W., Fan, J., Chen, M., Guan, S., Sawcer, D., Bokoch, G. M., & Woodley, D. T. (2004). Mechanism of human dermal fibroblast migration driven by type I collagen and platelet-derived growth factor-BB. *Molecular biology of the cell, 15*(1), 294-309.

Lieber, A. R. G. a. R. L. (2011). Structure and function of the skeletal muscle extracellular matrix. *Muscle Nerve, 44*, 318-331. doi:10.1002/mus.22094

O'brien, F. J. (2011). Biomaterials & scaffolds for tissue engineering. *Materials today, 14*(3), 88-95.

Ohto-Fujita, E., Konno, T., Shimizu, M., Ishihara, K., Sugitate, T., Miyake, J., . . . Hasebe, Y. (2011). Hydrolyzed eggshell membrane immobilized on phosphorylcholine polymer supplies extracellular matrix environment for human dermal fibroblasts. *Cell and tissue research, 345*(1), 177-190.

Ostrovidov, S., Hosseini, V., Ahadian, S., Fujie, T., Parthiban, S. P., Ramalingam, M., . . . Khademhosseini, A. (2014). Skeletal muscle tissue engineering: methods to form skeletal myotubes and their applications. *Tissue Engineering Part B: Reviews, 20*(5), 403-436.

Pierce LDH Cytotoxicity Assay Kit. (last accessed 2018).

Riessen, R., Isner, J. M., Blessing, E., Loushin, C., Nikol, S., & Wight, T. N. (1994). Regional differences in the distribution of the proteoglycans biglycan and decorin in the extracellular matrix of atherosclerotic and restenotic human coronary arteries. *The American journal of pathology, 144*(5), 962.

Roche. (2012). Cytotoxicity Detection Kit(LDH).

Rosso, F., Giordano, A., Barbarisi, M., & Barbarisi, A. (2004). From cell–ECM interactions to tissue engineering. *Journal of cellular physiology, 199*(2), 174-180.

Rønning, S. B., Pedersen, M. E., Andersen, P. V., & Hollung, K. (2013). The combination of glycosaminoglycans and fibrous proteins improves cell proliferation and early differentiation of bovine primary skeletal muscle cells. *Differentiation, 86*(1-2), 13-22.

Sabourin, L. A., & Rudnicki, M. A. (2000). The molecular regulation of myogenesis. *Clinical genetics, 57*(1), 16-25.

Sah, M. K., & Rath, S. N. (2016). Soluble eggshell membrane: A natural protein to improve the properties of biomaterials used for tissue engineering applications. *Materials Science and Engineering: C, 67*, 807-821.

Schaefer, L., & Schaefer, R. M. (2010). Proteoglycans: from structural compounds to signaling molecules. *Cell and tissue research, 339*(1), 237.

Schmittgen, T. D., & Livak, K. J. (2008). Analyzing real-time PCR data by the comparative C T method. *Nature protocols, 3*(6), 1101.

Sousa-Victor, P., Gutarra, S., García-Prat, L., Rodriguez-Ubreva, J., Ortet, L., Ruiz-Bonilla, V., . . . Serrano, A. L. (2014). Geriatric muscle stem cells switch reversible quiescence into senescence. *Nature, 506*(7488), 316.

Structure of the skeletal muscle (accessed 2018). *Muscular system.*

Syverud, B. C., Lee, J. D., VanDusen, K. W., & Larkin, L. M. (2014). Isolation and purification of satellite cells for skeletal muscle tissue engineering. *Journal of regenerative medicine, 3*(2).

Theocharis, A. D., Skandalis, S. S., Gialeli, C., & Karamanos, N. K. (2016). Extracellular matrix structure. *Advanced drug delivery reviews, 97*, 4-27.

Tidball, J. G. (2005). Inflammatory processes in muscle injury and repair. *American Journal of Physiology-Regulatory, Integrative and Comparative Physiology, 288*(2), R345-R353.

Tsai, W., Yang, J., Lai, C., Cheng, Y., Lin, C., & Yeh, C. (2006). Characterization and adsorption properties of eggshells and eggshell membrane. *Bioresource technology, 97*(3), 488-493.

Verdijk, L. B., Snijders, T., Drost, M., Delhaas, T., Kadi, F., & Van Loon, L. J. (2014). Satellite cells in human skeletal muscle; from birth to old age. *Age, 36*(2), 545-557.

Vuong, T. T., Rønning, S. B., Suso, H.-P., Schmidt, R., Prydz, K., Lundström, M., . . . Pedersen, M. E. (2017). The extracellular matrix of eggshell displays anti-inflammatory activities through NF-κB in LPS-triggered human immune cells. *Journal of inflammation research, 10*, 83.

Wilhelmsen, C. R. (2017). *Eggshell membrane as an extracellular matrix environment for enhancing wound healing*. Eggshell membrane as an extracellular matrix environment for enhancing wound healing. NMBU.

Yablonka-Reuveni, Z. (1995). Development and postnatal regulation of adult myoblasts. *Microscopy research and technique, 30*(5), 366-380.

Yarrow, J. C., Perlman, Z. E., Westwood, N. J., & Mitchison, T. J. (2004). A high-throughput cell migration assay using scratch wound healing, a comparison of image-based readout methods. *BMC biotechnology, 4*(1), 21.

Appendix

Change in expression was calculated by obtaining data from real time-PCR and using TATA as reference gene to calculate fold change for myoblast cells interacting with coated ESM at concentrations of 0.01 mg/ml and 0.0001 mg/ml during proliferation and differentiation. The values for each graph were calculated using the ΔΔct value to estimate fold change, with fold change values equaling no change (1.0) decrease (<1.0) and increase (>1.0) in expression. Significant values were calculated using the p-value with *(p-value <0.05) and ** (p-value<0.01). Fold change and significant values were calculated for MyoD, myogenin, decorin

MyoD

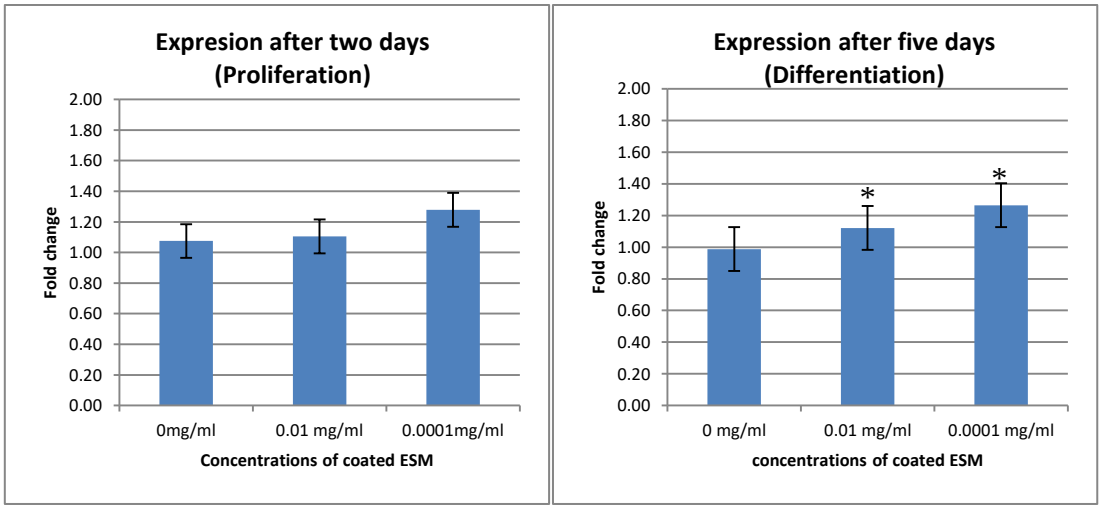

Myogenin

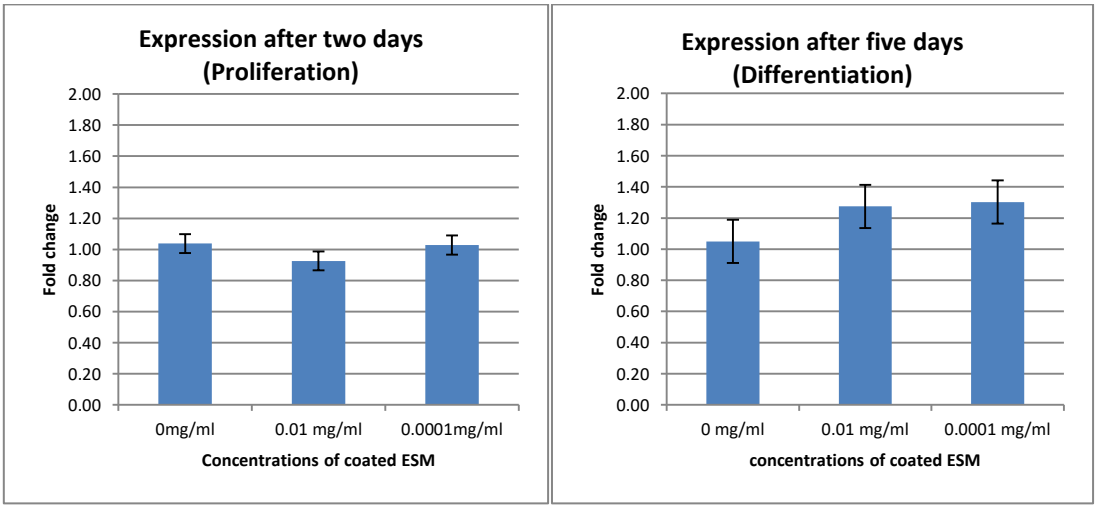

Decorin

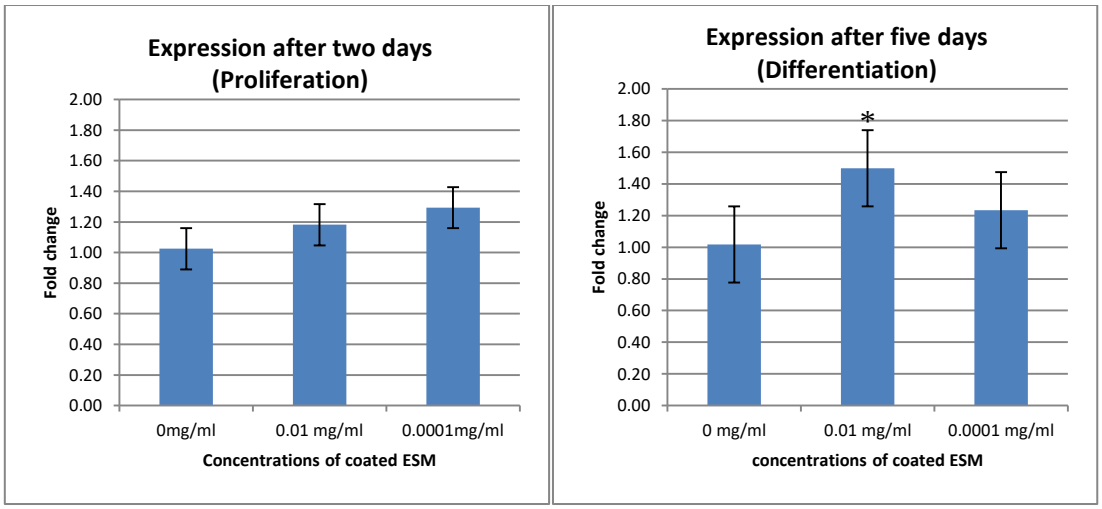

Collagen

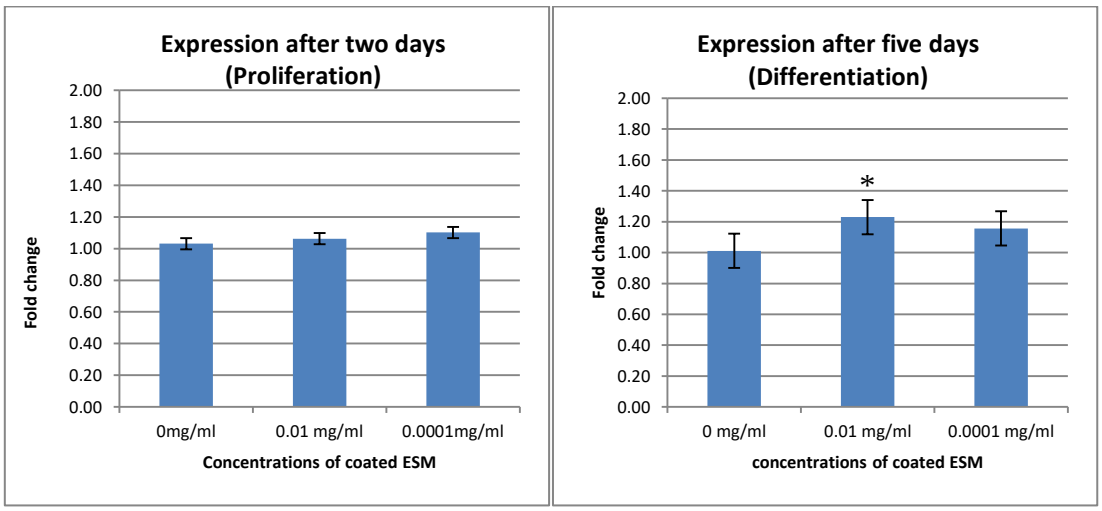

Biglycan

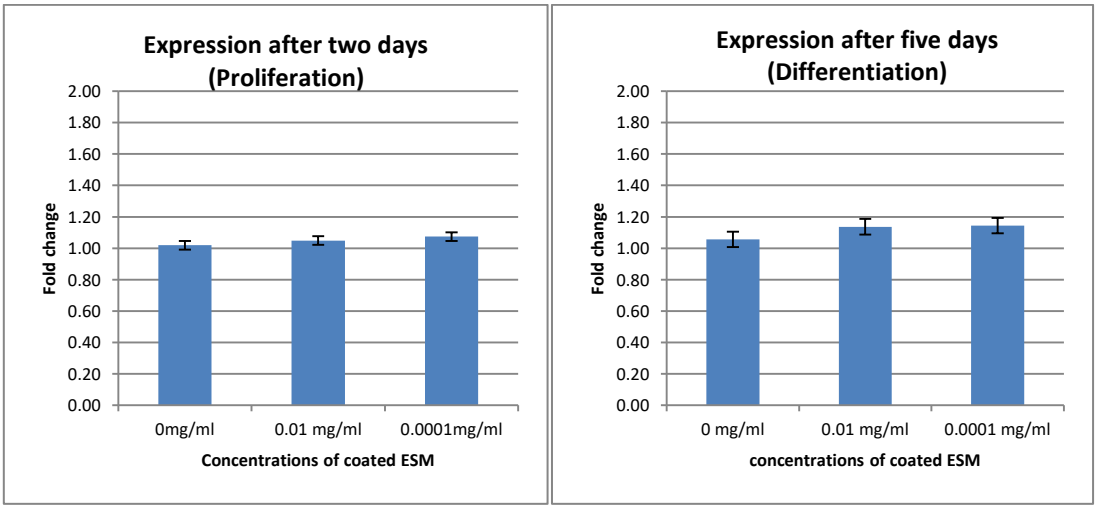

Norges miljø- og biovitenskapelige universitet
Noregs miljø- og biovitskapelege universitet
Norwegian University of Life Sciences

Postboks 5003
NO-1432 Ås
Norway